Electronic Supplementary Information (ESI)

2-Dimensional Rare Earth Metal-Organic Frameworks based on a hexanuclear secondary building unit as efficient detectors for vapours of nitroaromatics and volatile organic compounds

Nikos Panagiotou[a], Francisco García Moscoso[b], Tânia Lopes-Costa[b], José María Pedrosa[b]*, Anastasios J. Tasiopoulos[a]*

[a]Department of Chemistry, University of Cyprus, 1678 Nicosia, Cyprus. E-mail: atasio@ucy.ac.cy

[b]Department of Physical, Chemical and Natural Systems, Universidad Pablo de Olavide, 41013 Seville, Spain.

Table of Contents

Experimental Part

Synthesis of analytes used in sensing studies

2,4,6-Trinitrotoluene

TNT was synthesized by mononitration of DNT with a mixture of concentrated sulfuric and fuming nitric acid in a 5:2 ratio (V/V). The DNT:nitric acid molar *ratio* is calculated to be 1:2. The flask is slowly heated to 110 ºC, and the reaction is allowed to occur for 1 h. The mixture is cooled to 80 ºC and then distilled water is gently added. The mixture is transferred to a separation funnel, and the upper layer is separated and washed sequentially with distilled water and sodium carbonate solution. The so-obtained solid is recrystallized in an ethanol/toluene (95%, 5%) solution, weighted and purified with sodium sulfite solution with a TNT:sulfite molar ratio of 10:1. A small aliquot is dissolved in ethanol and analyzed with an ion trap spectrometer (HCT, Bruker-Daltonics). The mass (MS) and fragmentation (MS/MS) spectra recorded in positive mode is consistent with the results reported in the literature.[1]

Triacetone triperoxide

A 1:1 molar ratio mixture of acetone and aqueous 30% wt hydrogen peroxide was placed in an ice bath to keep the temperature of the mixture at 0-5ºC all the time. Under magnetic stirring, 37% wt HCl (1.3 equivalents) was added drop by drop. After 1 hour, a white precipitate had formed. Next, the product was filtered, washed with cold distilled water, and dried in air. Finally, the product was recrystallized in dichloromethane and characterized by mass spectrometry which proved the obtention of the desired product.[2]

Table S1: Selected Crystal Data for **UCY-15**(RE).

Compound	**UCY-15**(Y)	**UCY-15**(Eu)	**UCY-15**(Gd)	**UCY-15**(Tb)	**UCY-15**(Dy)	**UCY-15**(Ho)
Empirical formula	$C_{28}H_{16}NO_{22}S_2Y_3$	$C_{28}H_{16}NO_{22}S_2Eu_3$	$C_{28}H_{16}NO_{22}S_2Gd_3$	$C_{28}H_{16}NO_{22}S_2Tb_3$	$C_{28}H_{16}NO_{22}S_2Dy_3$	$C_{28}H_{16}NO_{22}S_2Ho_3$
Formula weight	1049.27	1238.45	1254.29	1259.3	1270.04	1277.33
Temperature / K	104(2)	105(4)	102.8(9)	103.8(9)	103.8(8)	105(1)
Wavelength / Å	1.54184	1.54184	1.54184	1.54184	1.54184	1.54184
Crystal system	Monoclinic	Monoclinic	Monoclinic	Monoclinic	Monoclinic	Monoclinic
Space group	*C* 2/*m*	*C* 2/*m*	*C* 2/*m*	*C* 2/*m*	*C* 2/*m*	*C* 2/*m*
a / Å	29.232(8)	29.457(2)	29.272(2)	29.298(6)	29.243(1)	29.360(9)
b / Å	18.441(8)	18.607(8)	18.611(1)	18.510(4)	18.498(1)	18.475(6)
c / Å	14.630(4)	14.691(1)	14.579(6)	14.423(3)	14.460(3)	14.691(6)
$\alpha = \gamma$ / °	90	90	90	90	90	90
β / °	104.3(3)	103.8(5)	103.9(5)	103.5(2)	103.8(2)	104.3(3)
Volume / Å^3	7642.3(5)	7819.7(8)	7708.8(7)	7605.3(3)	7598.0(3)	7721.7(4)
Z	4	4	4	4	4	4
$d_{calc.}$/ g/cm^3	0.912	1.054	1.078	1.1	1.11	1.099
Absorption coefficient / mm^{-1}	3.885	17.869	17.333	14.381	16.448	6.394
F(000)	2064	2352	2364	2376	2388	2400
Reflections collected	14335	14902	17267	15142	14568	23966
Independent reflections	6989	7205	7786	7006	7010	7092
Completeness to θ = 66.999°	99.20% [R(int) = 0.0594]	99.80% [R(int) = 0.0559]	99.80% [R(int) = 0.0741]	99.90% [R(int) = 0.0344]	99.80% [R(int) = 0.0403]	99.50% [R(int) = 0.0416]
Data / restraints / parameters	6989 / 16 / 262	7205 / 16 / 262	7786 / 16 / 262	7006 / 25 / 262	6997 / 22 / 262	7092 / 1 / 262
Goodness-of-fit	1.068	0.98	1.039	1.01	1.027	1.083
Final R indices [I > 2σ(I)]	$R_{obs.}$ = 0.0849, $wR_{obs.}$ = 0.2560	$R_{obs.}$ = 0.0680, $wR_{obs.}$= 0.1867	$R_{obs.}$ = 0.0845, $wR_{obs.}$ = 0.2423	$R_{obs.}$ = 0.0479, $wR_{obs.}$ = 0.1359	$R_{obs.}$ = 0.0513, $wR_{obs.}$ = 0.1467	$R_{obs.}$ = 0.0588, $wR_{obs.}$ = 0.1792
R indices [all data]	R_{all} = 0.1199, wR_{all} = 0.2814	R_{all} = 0.0790, wR_{all} = 0.1951	R_{all} = 0.1119, wR_{all} = 0.2833	R_{all} = 0.0565, wR_{all} = 0.1402	R_{all} = 0.0583, wR_{all} = 0.1517	R_{all} = 0.0655, wR_{all} = 0.1893

[a] $R = \Sigma||F_o|-|F_c|| / \Sigma|F_o|$, $wR = \{\Sigma[w(|F_o|^2 - |F_c|^2)^2] / \Sigma[w(|F_o|^4)]\}^{1/2}$ and
[b] $w=1/[\sigma^2(F_o^2)+(mP)^2+nP]$ where $P=(Fo^2+2Fc^2)/3$ and m and n are constants

Physical Measurements/Characterization of UCY-15(RE) (RE: Y, Eu, Gd, Tb, Dy, Ho, Er)

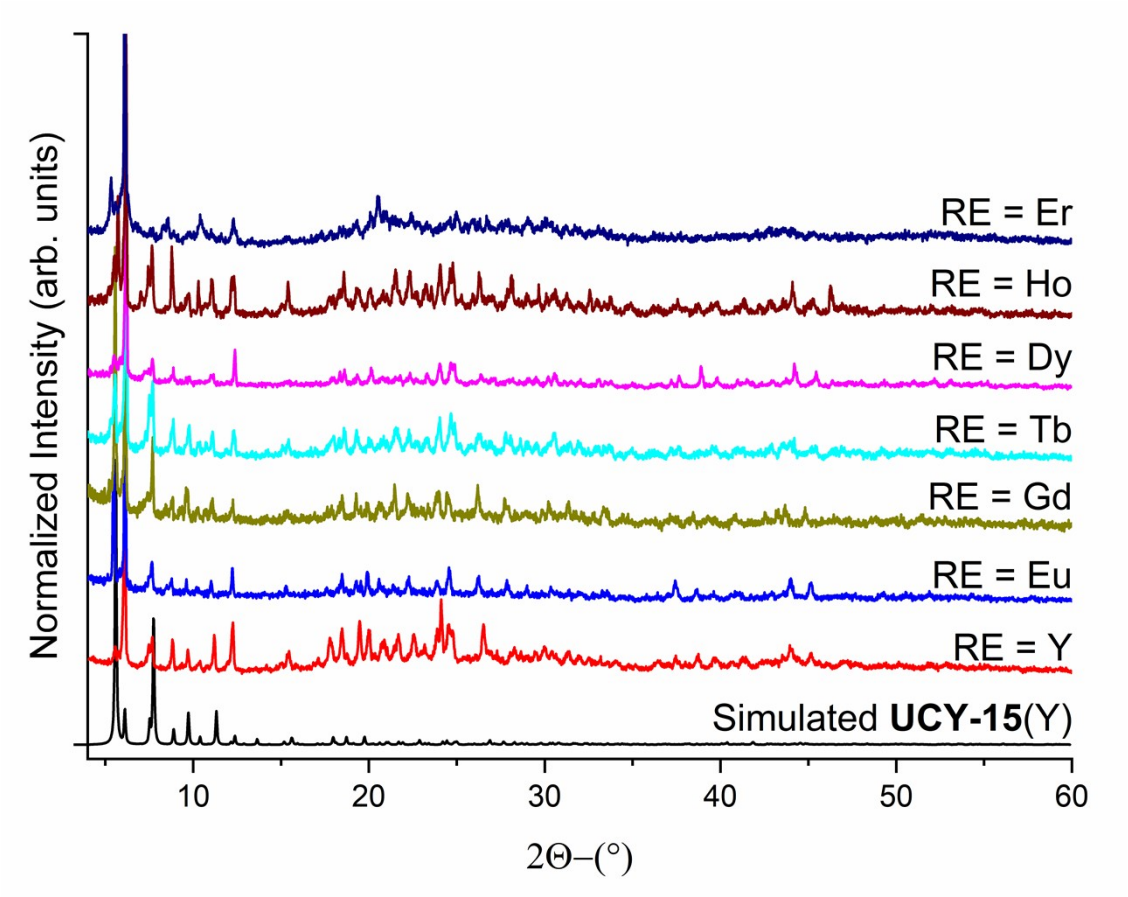

Figure S1: Powder X-ray diffraction pattern of the as synthesized compounds **UCY-15**(RE), along with the simulated pattern of **UCY-15**(Y) from the single crystal data.

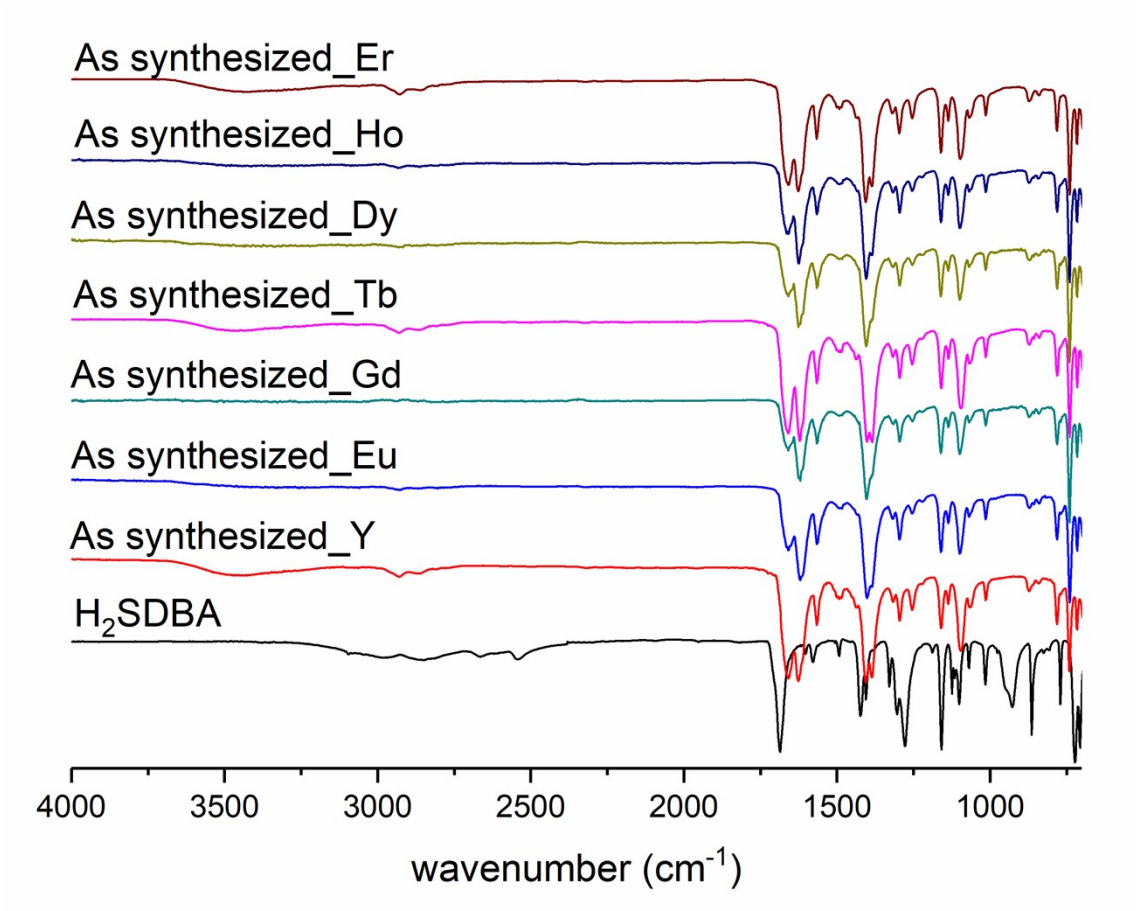

Figure S2: IR spectra of H_2SDBA and the as synthesized compounds **UCY-15**(RE).

Functional Group	IR frequency (cm^{-1})	
	H_2SDBA	**UCY-15(RE)**
ν(O-H), H_2O	-	~3400
ν(=C-H)-p	3099, 864	866
ν(-CH_3 DMF)	-	2927, 2852
ν(C=O, DMF)	-	1660
$\nu(C=O)_{ant}$	1685	1630
$\nu(C=O)_{sym}$	-	1406
ν(N-O), NO_3^-	-	1384
$\nu(S=O)_{ant}$	1278	1296
$\nu(S=O)_{sym}$	1159	1161

Table S2: IR peaks assignment.

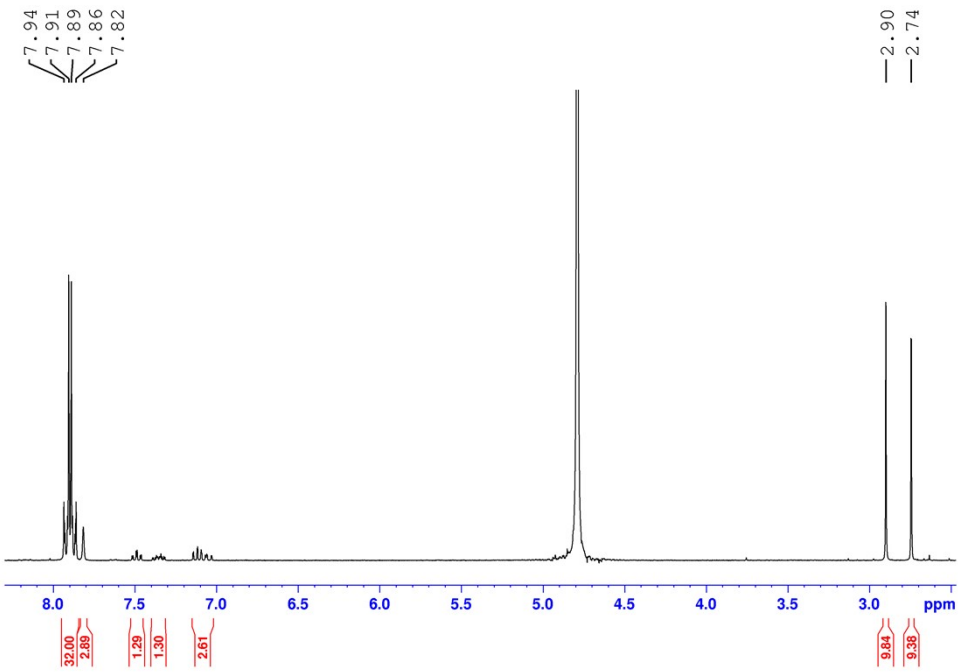

Figure S3: ^{1}H-NMR spectrum of as synthesized **UCY-15**(Y) digested in 0.5M KOH in D_2O. These data indicate the presence of the organic ligand $SDBA^{2-}$ as well as HFBA and DMF molecules in **UCY-15**(Y). ^{1}H NMR (D_2O): δ 4.79 (s, residual solvent peaks), δ 2.74 (s, 3H, C**H**$_3$, DMF), δ 2.9 (s, 3H, C**H**$_3$, DMF), δ 7.82 (s, H, C**HO**, DMF), δ 7.05-7.51 (m, 4H, Ar-**H**, FBA^{-}), δ 7.86-7.89 (d, 4H, Ar-**H**, $SDBA^{2-}$), δ 7.91 – 7.94 (d, 4H, Ar-**H**, $SDBA^{2-}$).

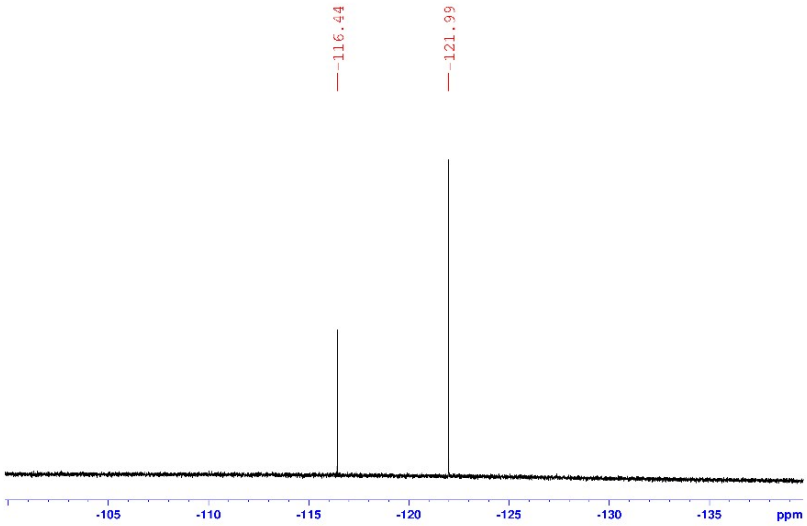

Figure S4: ^{19}F-NMR spectrum of as synthesized **UCY-15**(Y) digested in 0.5M KOH in D_2O. These data indicate the presence of the modulator HFBA and F^{-} anions in **UCY-15**(Y). ^{19}F NMR (D_2O): δ -116.44 (HFBA), δ -121.99 (F^{-}).[3,4]

Determination of the amount of F^- anions per $(Y^{3+})_6$ SBU in bulk UCY-15(Y) microcrystalline powder: In order to quantify the amount of F^- anions per $(Re^{3+})_6$ SBU ^{19}Fq-NMR measurements were performed. For this purpose, a trifluoroacetic acid (TFA) solution in D_2O was used as an external standard. Prior the ^{19}Fq-NMR experiment, the concentration of the trifluoroacetic acid (TFA) solution was determined using NaF solutions with known concentration. Afterwards microcrystalline powder of **UCY-15**(Y) (~ 10 – 15mg in each experiment) was digested in a 0.5M KOH solution and then 500 μL of the resulting solution was transferred to the NMR tube along with the microprobe tube containing the external standard (the known concentration trifluoroacetic acid (TFA) solution). The experiment was repeated three times.[5]

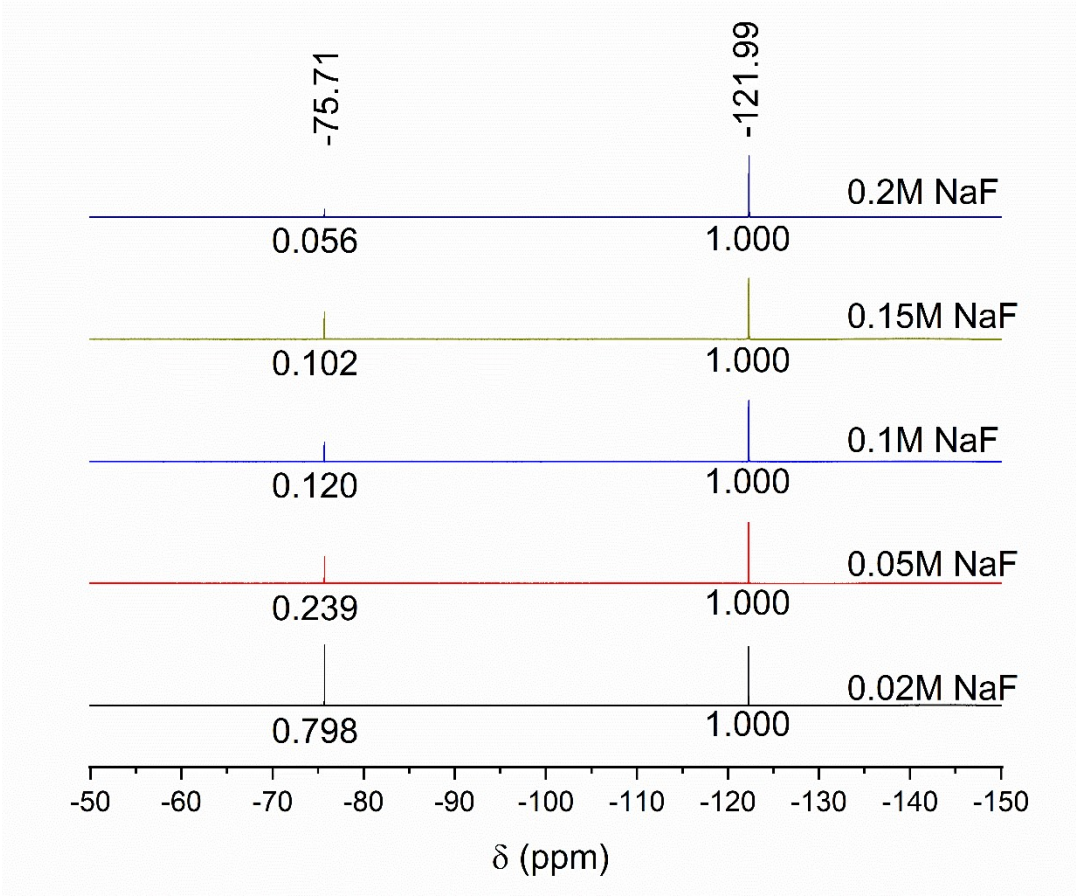

Figure S5: ^{19}Fq-NMR calibration spectra of the TFA solution external standard using NaF solutions of known concertation. TFA concentration was found equal to 4.4 ± 0.6mM. ^{19}F NMR (D_2O): δ -75.71 (TFA), δ -121.99 (F^-).

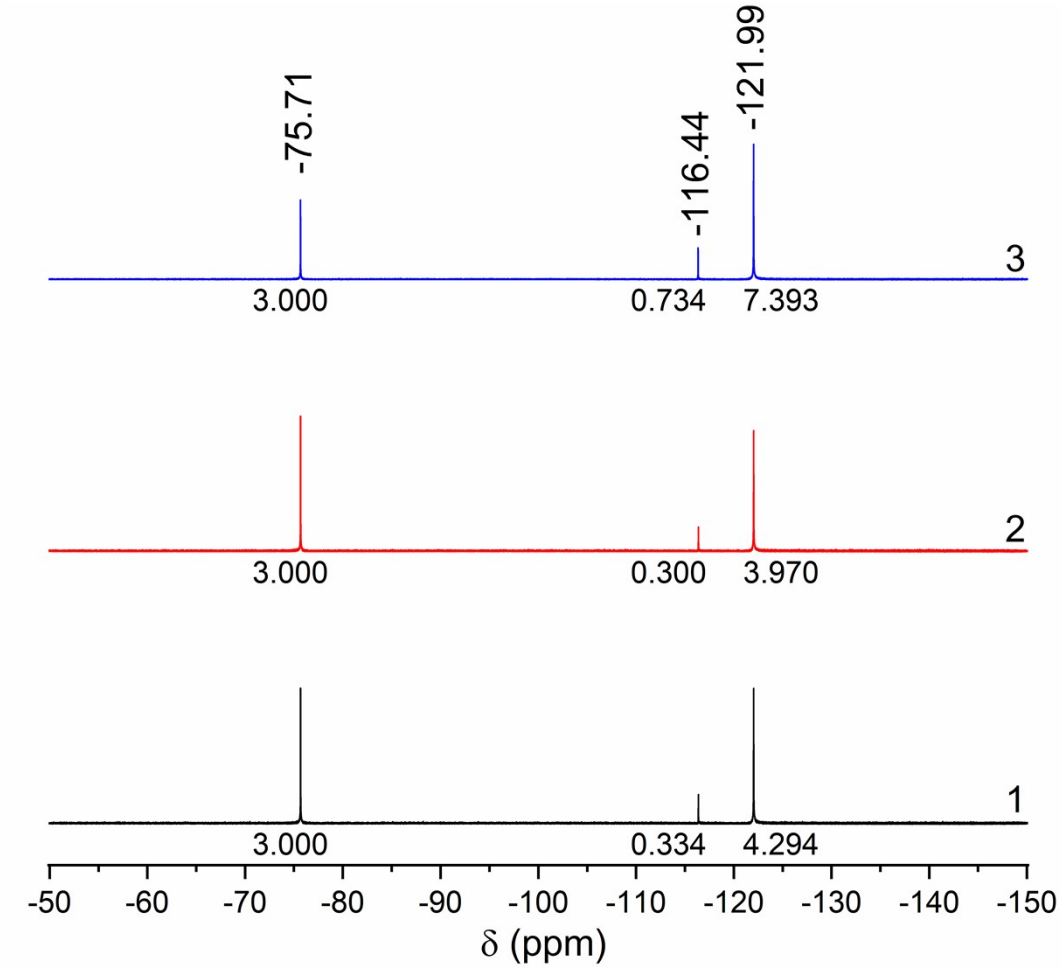

Figure S6: ^{19}Fq-NMR spectra of as synthesized **UCY-15**(Y) digested in 0.5M KOH in D_2O along with the TFA solution external standard. These studies indicated that **UCY-15**(Y) contains ~ 2.9 ± 0.4 F^- anions / $(Y^{3+})_6$ SBU. Moreover, the quantity of the trapped HFBA molecules was found to be ~ 0.29 ± 0.04 HFBA / $(Y^{3+})_6$ SBU. ^{19}F NMR (D_2O): δ -75.71 (TFA), δ -116.44 (FBA^-), δ -121.99 (F^-).

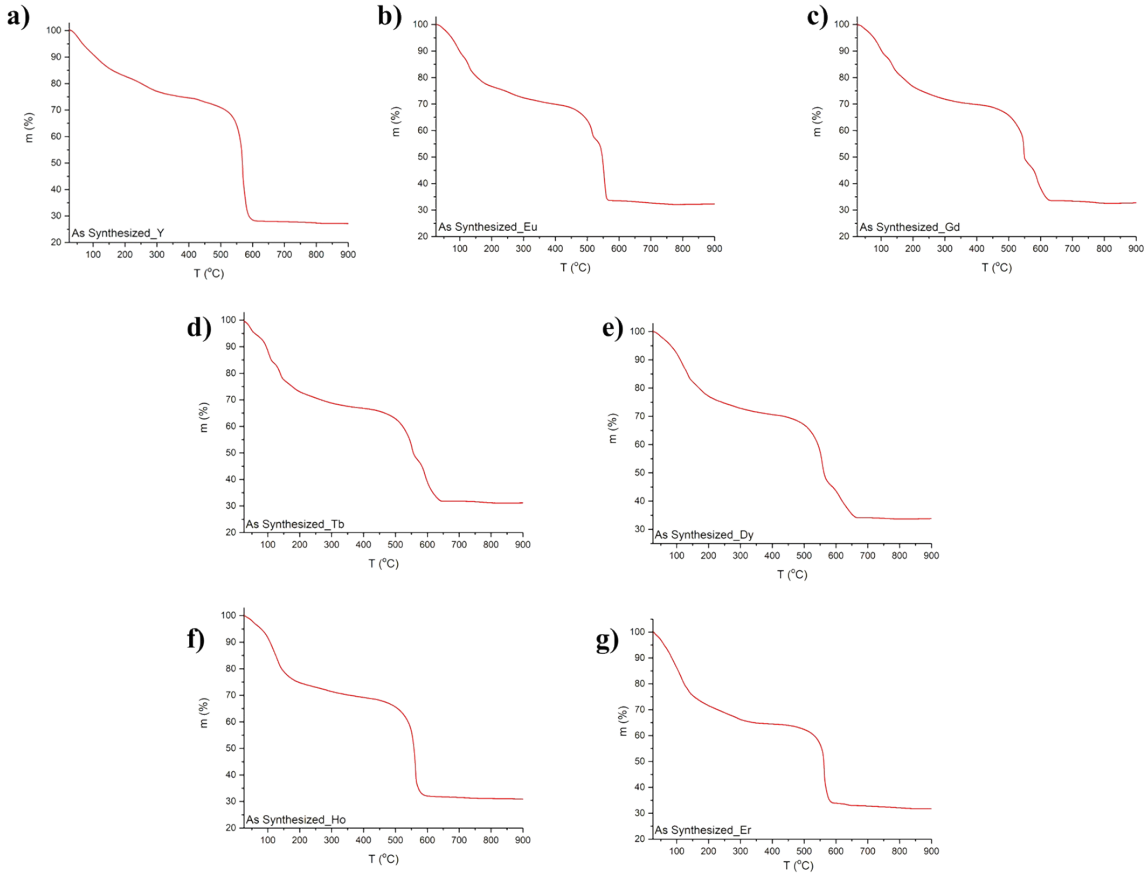

Figure S7: TGA graphs of the as synthesized compounds **UCY-15**(RE) ((a) RE = Y, (b) RE = Eu, (c) RE = Gd, (d) RE = Tb, (e) RE = Dy, (f) RE = Ho, (g) RE = Er). TG analysis reveals that the thermal decomposition of compounds **UCY-15**(RE) proceeds via a two-step process. The first step (until ~460-480°C) is attributed to the removal of the terminal water molecules and lattice DMF molecules. The second mass loss which is completed at ~650°C for **UCY-15**(RE) is attributed to the decomposition of the ligand OBA^{2-}. Lastly the residual mass at 900°C corresponds to the rare earth oxide of the corresponding RE^{III} ion. Details on calculated values for solvent removal and ligand decomposition along with the experimental values obtained from TG analysis are shown in Table S2.

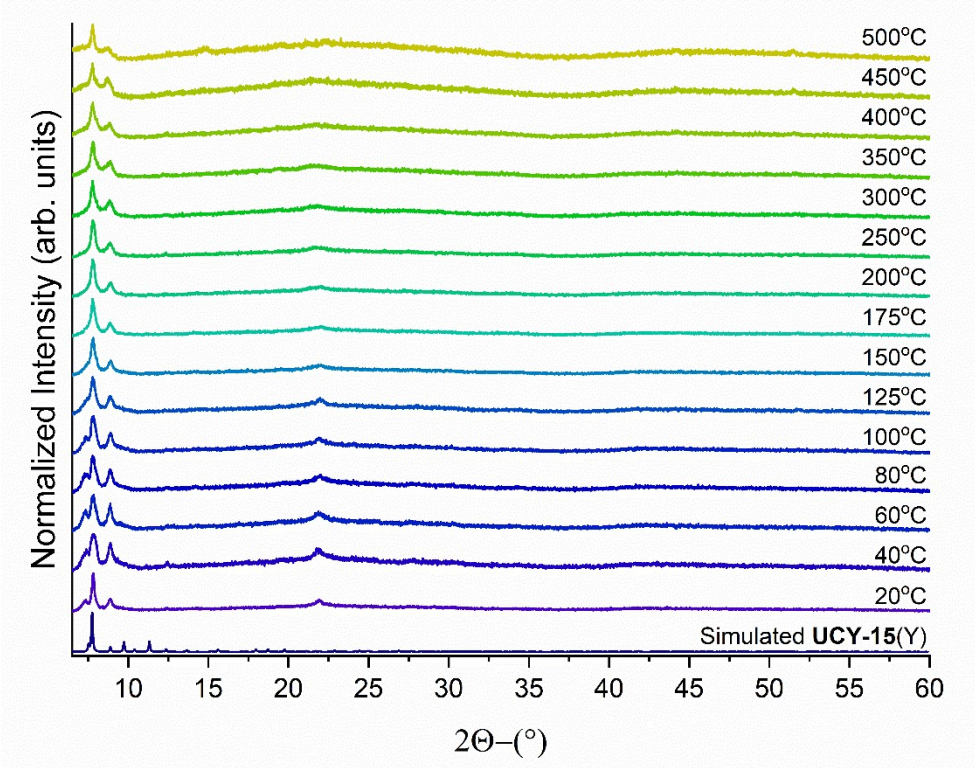

Figure S8: Variable temperature powder X-ray diffraction patterns of activated **UCY-15**(Y).

Table S3: Calculated values for solvent removal and ligand combustion along with the experimental values obtained from TG analysis for the as synthesized compounds **UCY-15**(RE).

Compound	Lattice Solvent Removal			Ligand Combustion		Residual Oxide		
	Temperature (°C)	Experimental (Calculated) (%)	xDMF	Temperature (°C)	Experimental (Calculated) (%)	Temperature (°C)	Experimental (Calculated) (%)	Formula
UCY-15(Y)	r.t. - 480	29 (29)	10	480 - 680	46 (47)	900	25 (24)	Y_2O_3
UCY-15(Eu)	r.t. - 460	31 (32)	14	460 - 630	37 (38)	900	32 (30)	Eu_2O_3
UCY-15(Gd)	r.t. - 460	32 (32)	14	460 - 650	37 (38)	900	31 (31)	Gd_2O_3
UCY-15(Tb)	r.t. - 460	35 (35)	16	460 - 690	33 (34)	900	32 (31)	Tb_4O_7
UCY-15(Dy)	r.t. - 470	32 (33)	15	470 - 680	36 (37)	900	32 (31)	Dy_2O_3
UCY-15(Ho)	r.t. - 470	33 (33)	15	470 - 650	36 (36)	900	31 (31)	Ho_2O_3
UCY-15(Er)	r.t. - 470	34 (35)	17	470 - 670	35 (35)	900	29 (30)	Er_2O_3

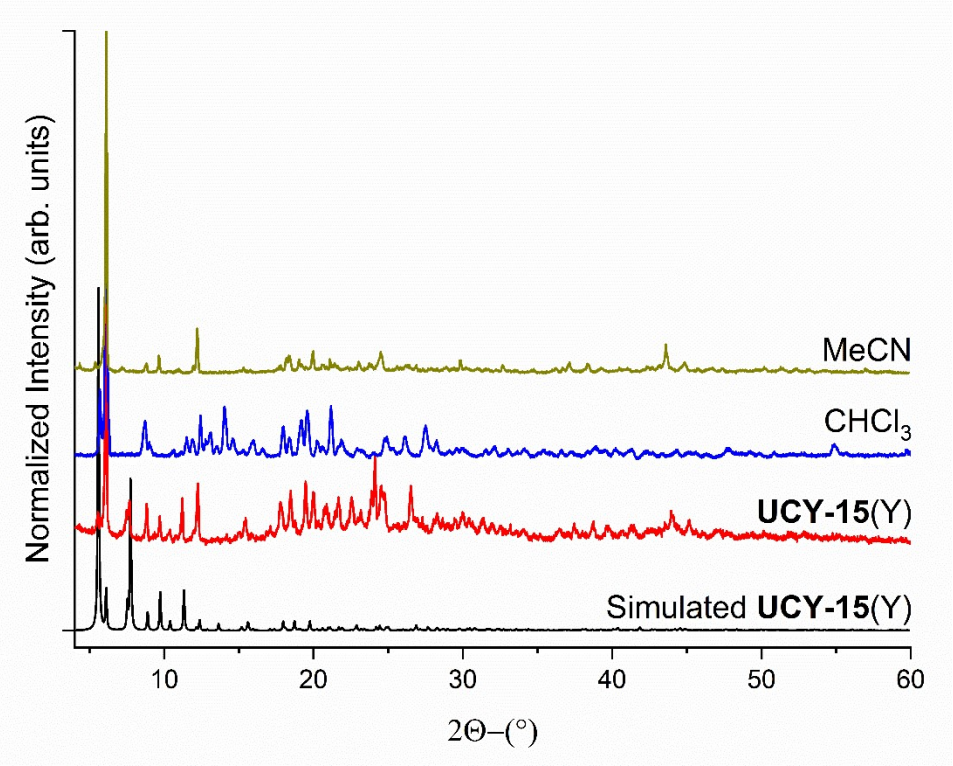

Figure S9: Powder X-ray diffraction patterns of as synthesized **UCY-15**(Y) treated (as described in the experimental part) in $CHCl_3$ and MeCN for 10 days.

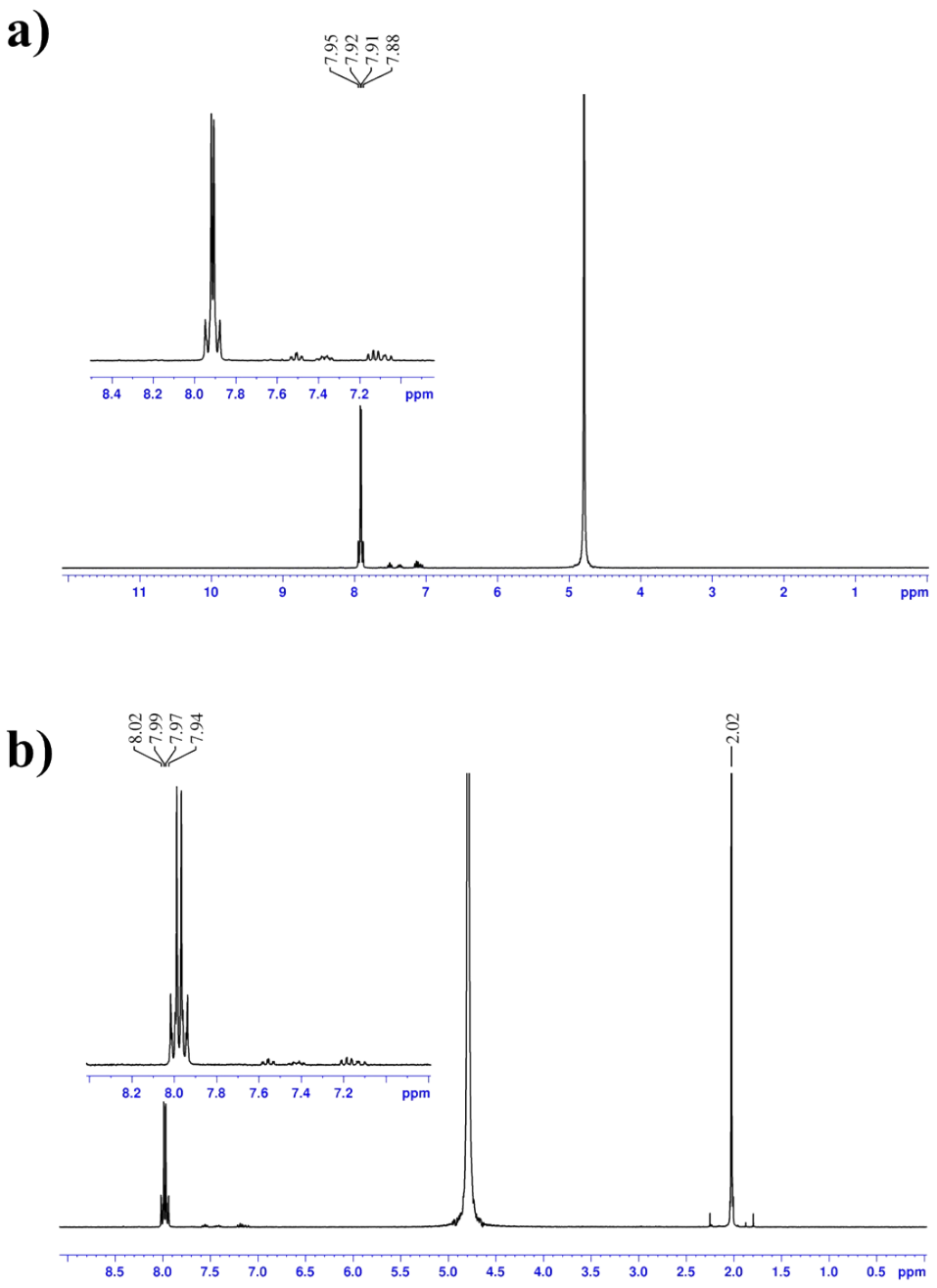

Figure S10: ^{1}H-NMR spectra of **UCY-15**(Y) after treatment with a) $CHCl_3$ and b) MeCN digested in 0.5M KOH in D_2O. These data indicate the absence of DMF molecules and the presence of the organic ligand $SDBA^{2-}$ as well as HFBA in **UCY-15**(Y). ^{1}H NMR (D_2O):a) δ 7.88-7.91 (d, 4H, Ar-**H**, $SDBA^{2-}$), δ 7.92 – 7.95 (d, 4H, Ar-**H**, $SDBA^{2-}$). b) δ 2.02 (s, 3H, C**H**$_3$CN), δ 4.9 (s, residual solvent peaks), δ 7.94 – 7.97 (d, 8H, Ar-**H**, $SDBA^{2-}$), δ 7.99 – 8.02 (d, 4H, Ar-**H**, $SDBA^{2-}$).

Gas Sorption Measurements

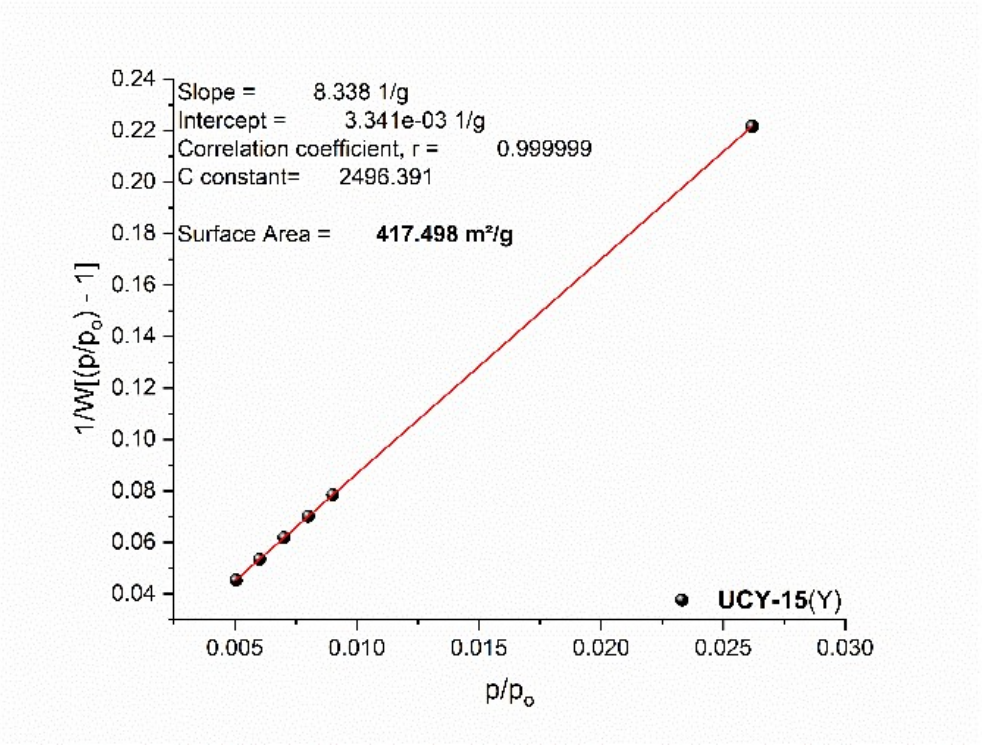

Figure S11: BET plot from N_2 adsorption isotherm at 77K for **UCY-15**(Y).

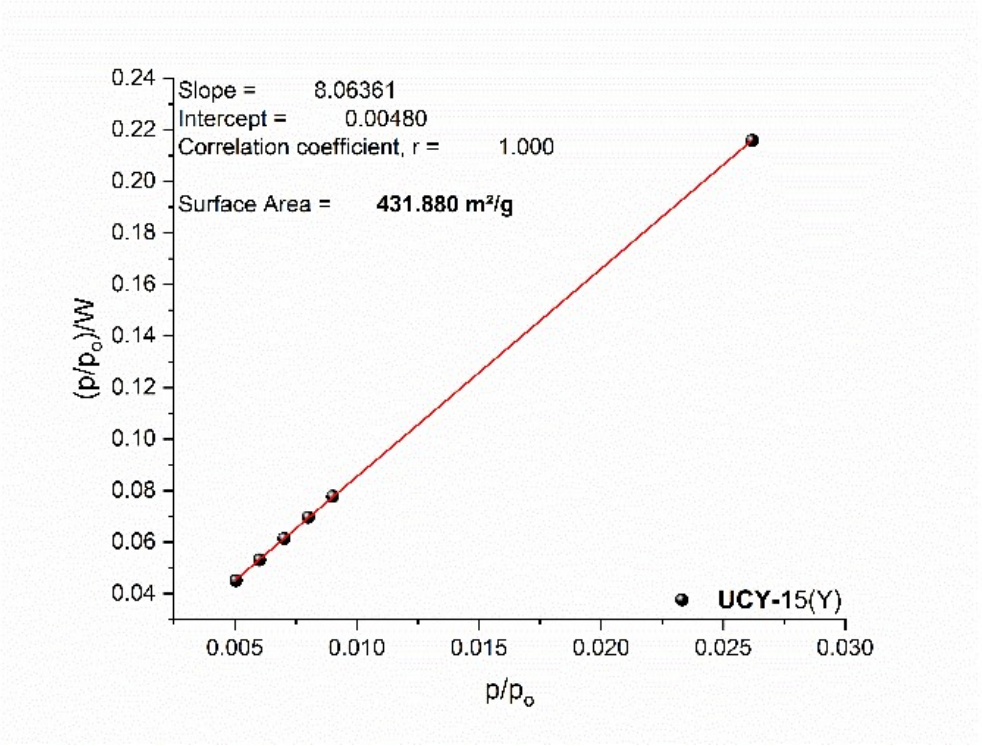

Figure S12: Langmuir plot from N_2 adsorption isotherm at 77K for **UCY-15**(Y).

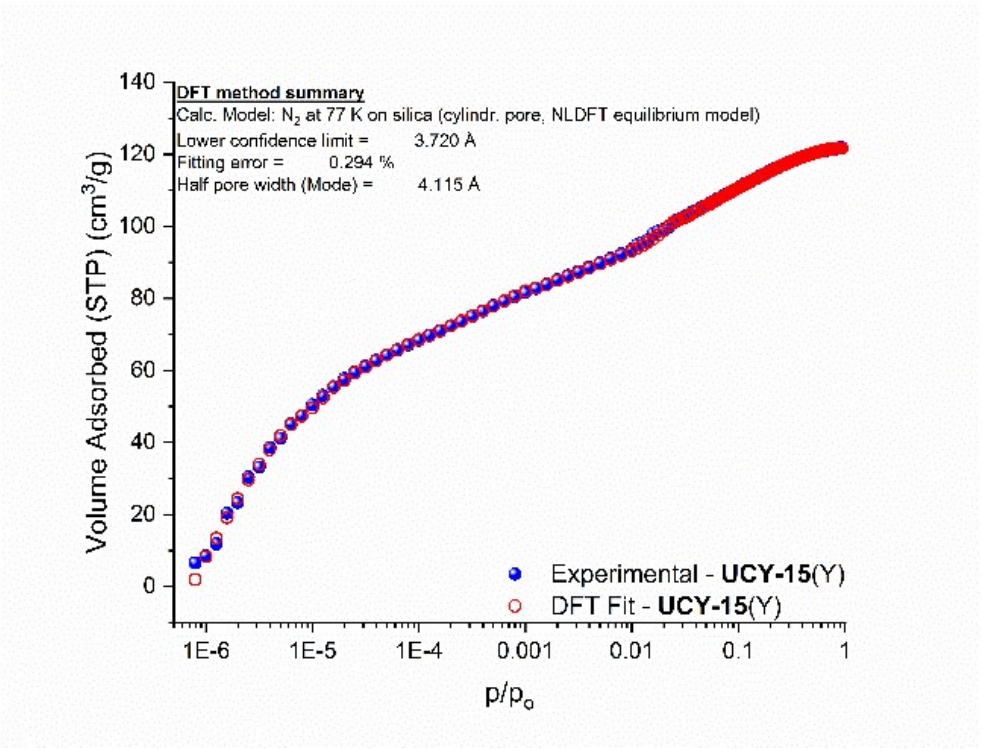

Figure S13: N_2 adsorption isotherm recorded at 77K and the corresponding NLDFT fitting for **UCY-15**(Y).

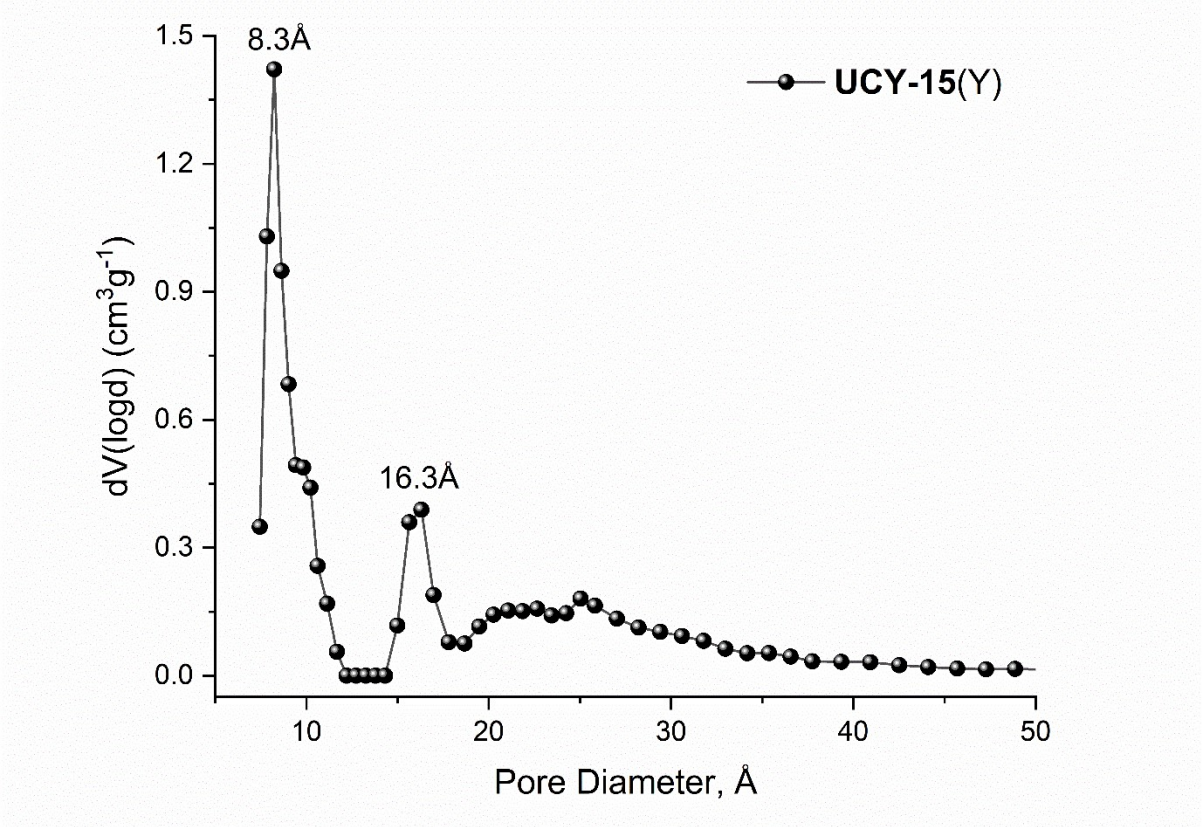

Figure S14: Pore size distribution curve of **UCY-15**(Y) calculated by NLDFT.

Low pressure CO_2, sorption isotherms, determination of heat of adsorption.

Heat of adsorption: To calculate heats of adsorptions, the corresponding adsorption isotherms at three different temperatures (273 K, 283K and 293 K) were simultaneously fitted using the virial type[6,7] Equation 1:

$$\ln P = \ln N + \frac{1}{T}\sum_{i=0}^{m} a_i N^i + \sum_{i=0}^{n} b_i N^i \qquad (1)$$

The heat of adsorption at zero coverage was calculated from Equation 2, where as a function of surface coverage, from Equation 3:

$$Q_{st} = -Ra_o \qquad (2)$$

$$Q_{st}(N) = -R\sum_{i=0}^{m} a_i N^i \qquad (3)$$

For the determination of the isosteric heat of adsorption using the Clausious - Clapeyron equation a commercially available software, ASiQwin (version 3.01) purchased from Quantachrome, was used.

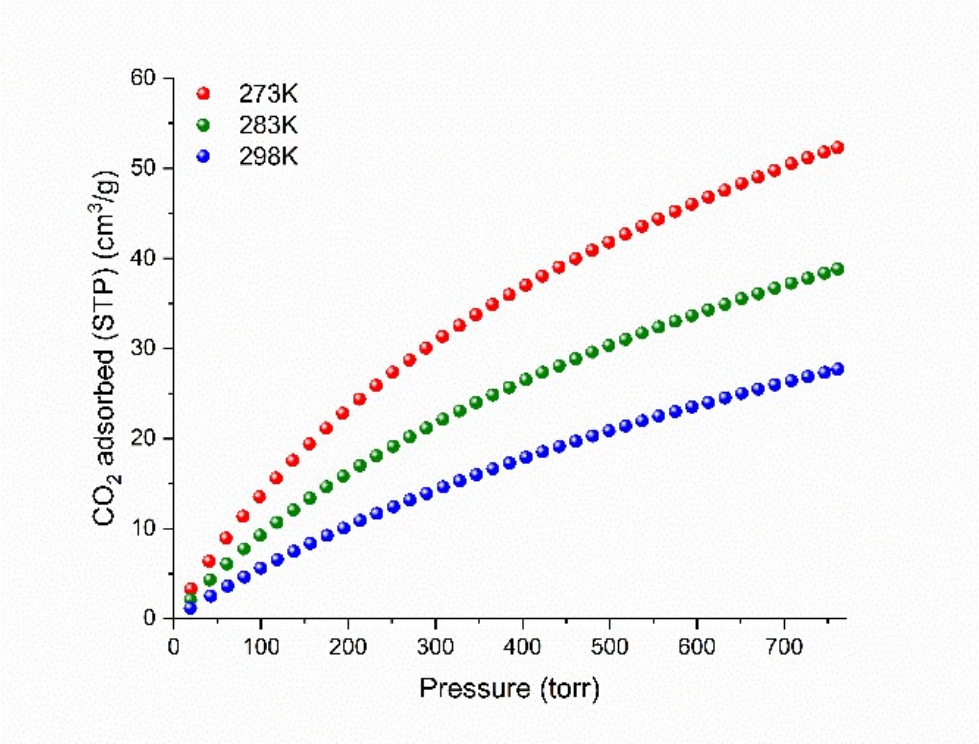

Figure S15: CO_2 adsorption isotherm of **UCY-15**(Y) at 273 K, 283K and 298 K.

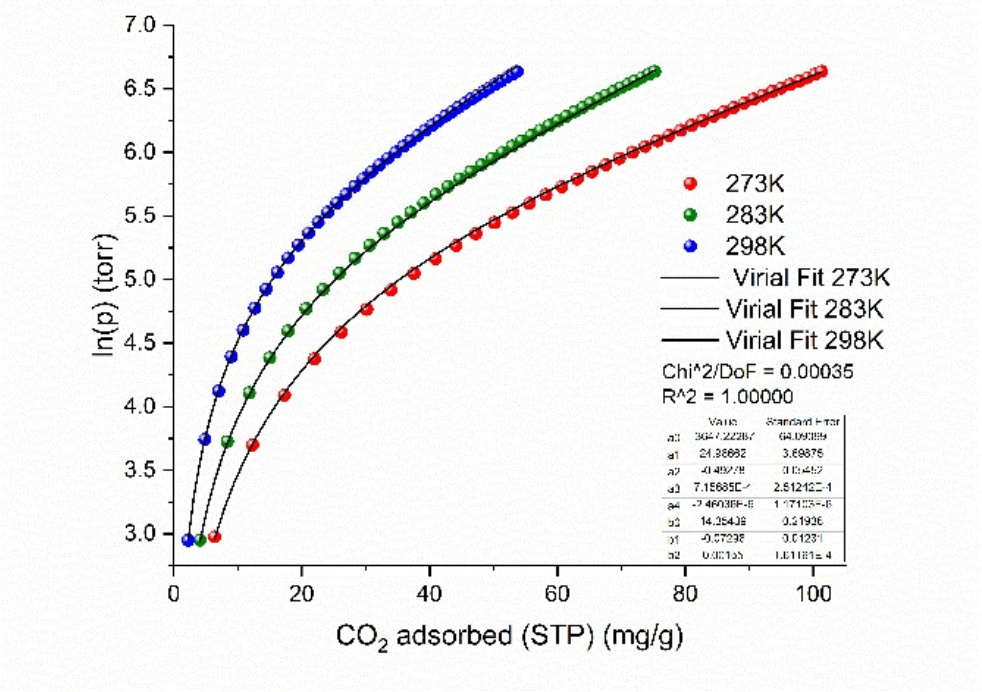

Figure S16: Virial type fitting of CO_2 adsorption isotherms of **UCY-15**(Y) at 273 K, 283 K and 298 K according to equation 1.

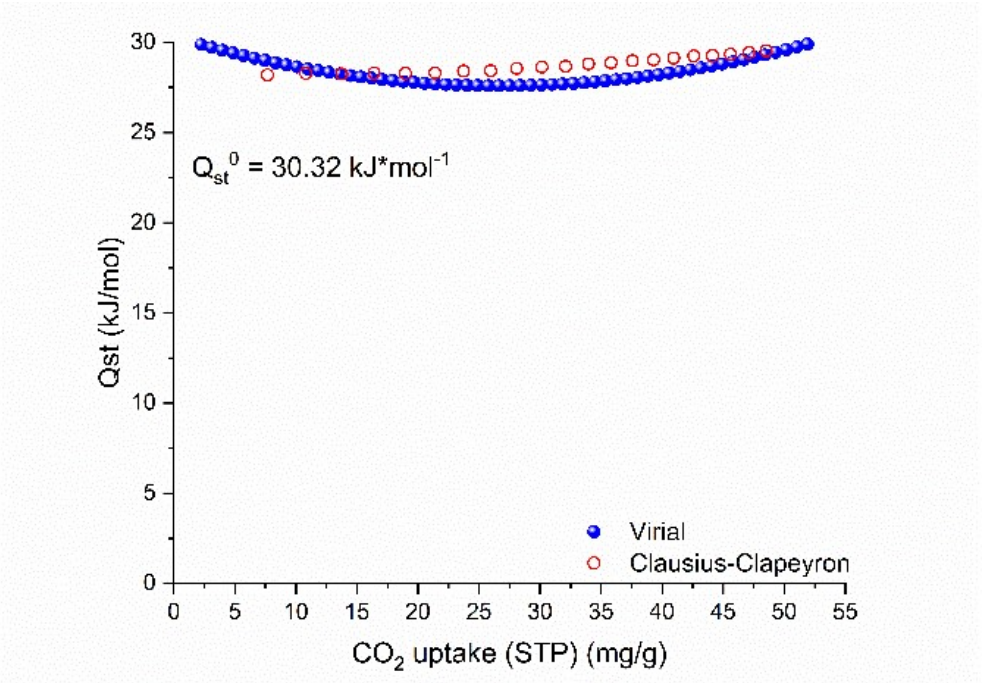

Figure S17: CO_2 isosteric heat of adsorption in **UCY-15**(Y) as a function of surface coverage.

Photoluminescence Studies

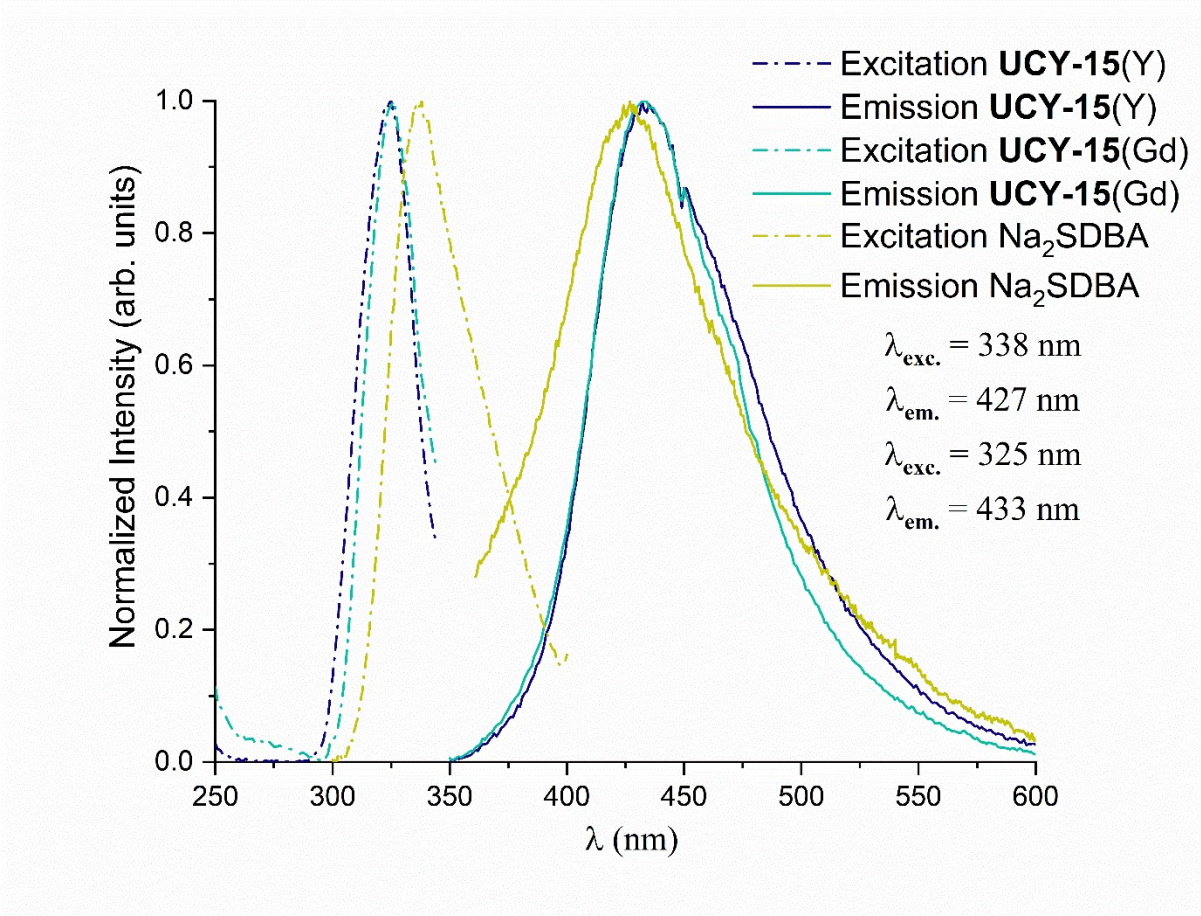

Figure S18: Normalized solid state excitation (λ_{em} = 433 nm, 23095cm^{-1}) and emission spectra (λ_{exc} = 325 nm) of the as synthesized compounds **UCY-15**(Y) and **UCY-15**(Gd) and excitation (λ_{em} = 427 nm) and emission spectra (λ_{exc} = 338 nm) of Na_2SDBA.

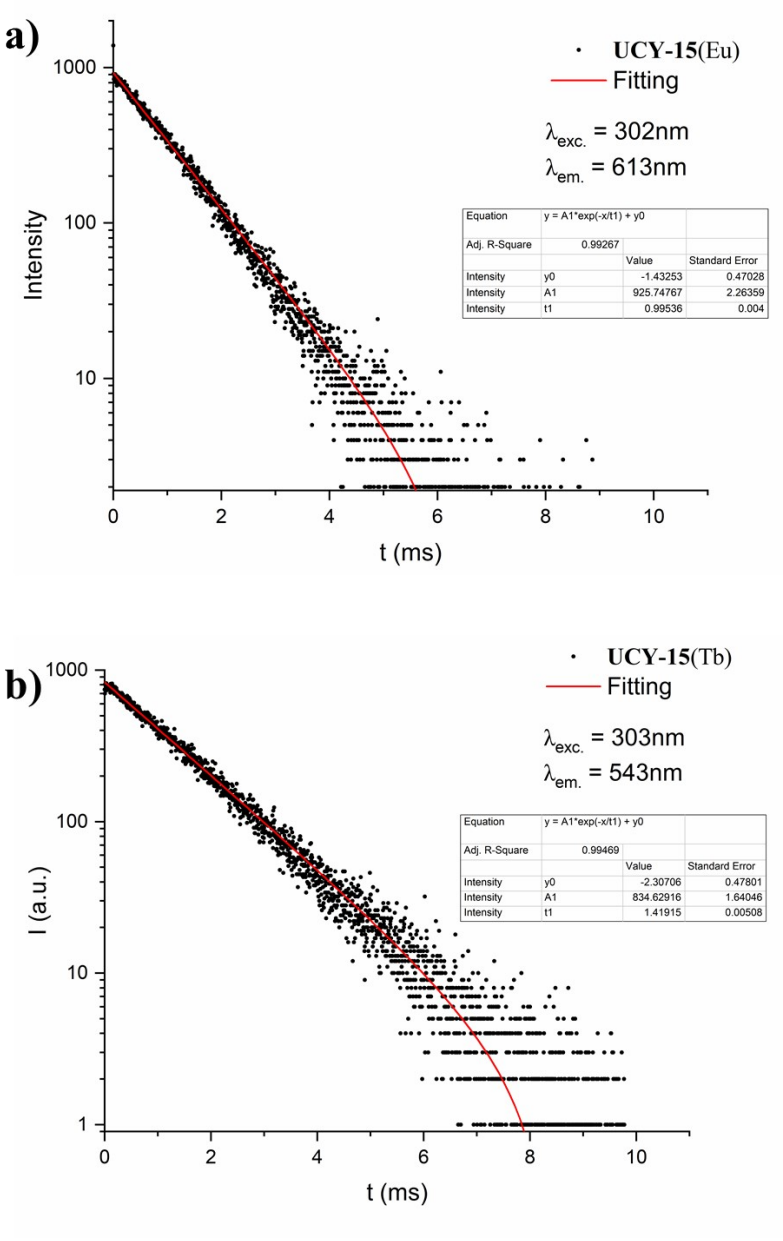

Figure S19: The decay of a) **UCY-15**(Eu) and b) **UCY-15**(Tb) at the indicated $\lambda_{em.}$.

In the case of **UCY-15**(Eu), it is possible to calculate the radiative lifetime, τ_R, of Eu^{3+} from the analysis of the lanthanide emission profile using eqn. (1)[8] where $A_{MD,0}$ is the probability of spontaneous emission of the $^5D_0 \rightarrow {}^7F_1$ transition *in vacuo* (14.65 s^{-1}), n is the refractive index of the material (estimated at 1.5[9]) and I_{tot}/I_{MD} is the ratio of the total integrated intensity of the Eu^{3+} emission to the area of the $^5D_0 \rightarrow {}^7F_1$ band. With the use of eqn. (2) we obtained a value of $\tau_R^{Eu} =$ 2.66 ms which led to an estimated value for the emission quantum yield of the Eu^{3+} ion, $\Phi_{Eu}^{Eu} = \tau_{obs}/\tau_R$, of *ca.* 38%.

$$\frac{1}{\tau_R} = A_{MD,0} n^3 \left(\frac{I_{tot}}{I_{MD}}\right) \quad (2)$$

Thin film characterisation and sensing studies

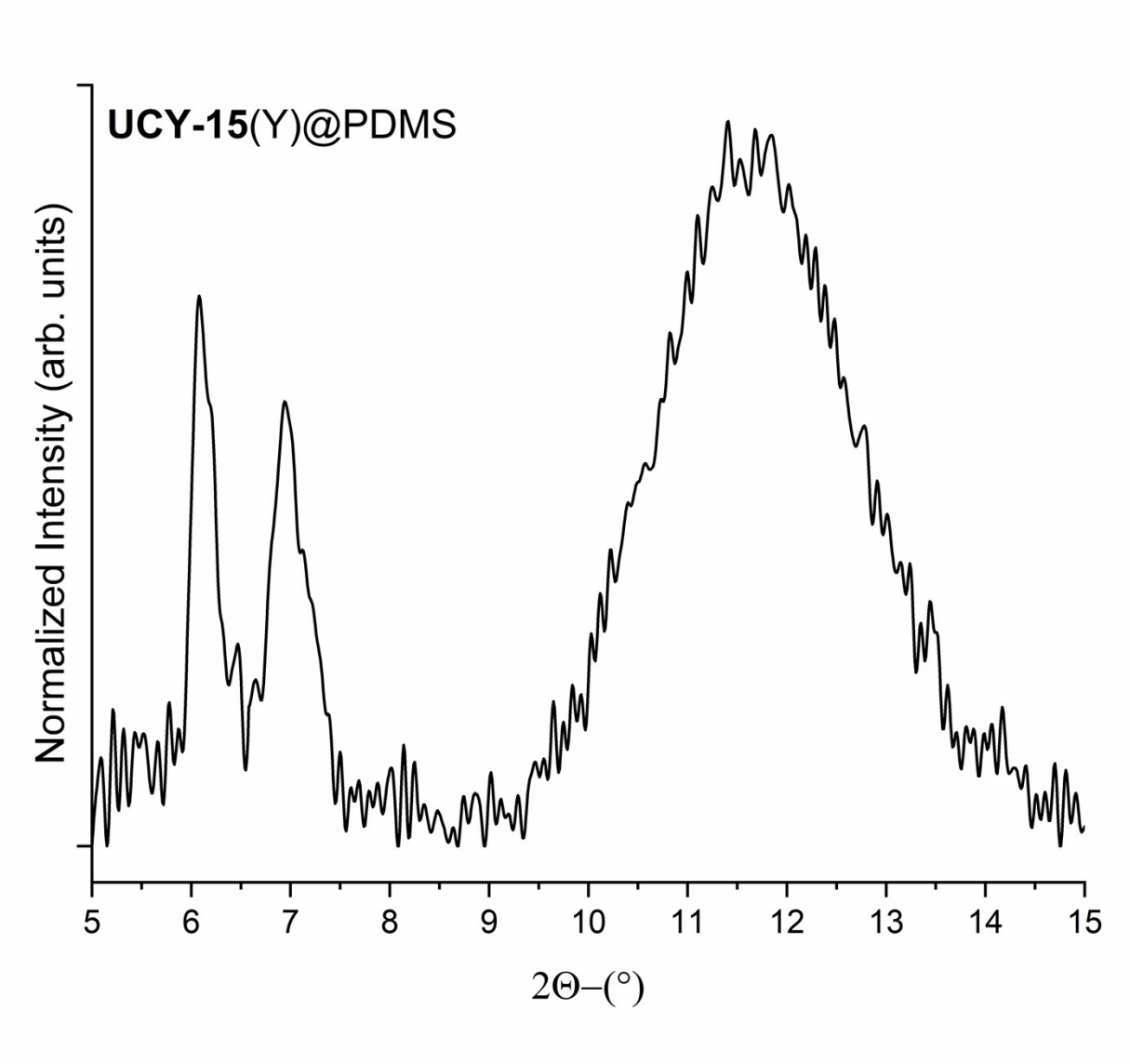

Figure S20: μ-XRD diffractogram of **UCY-15**(Y)@PDMS.

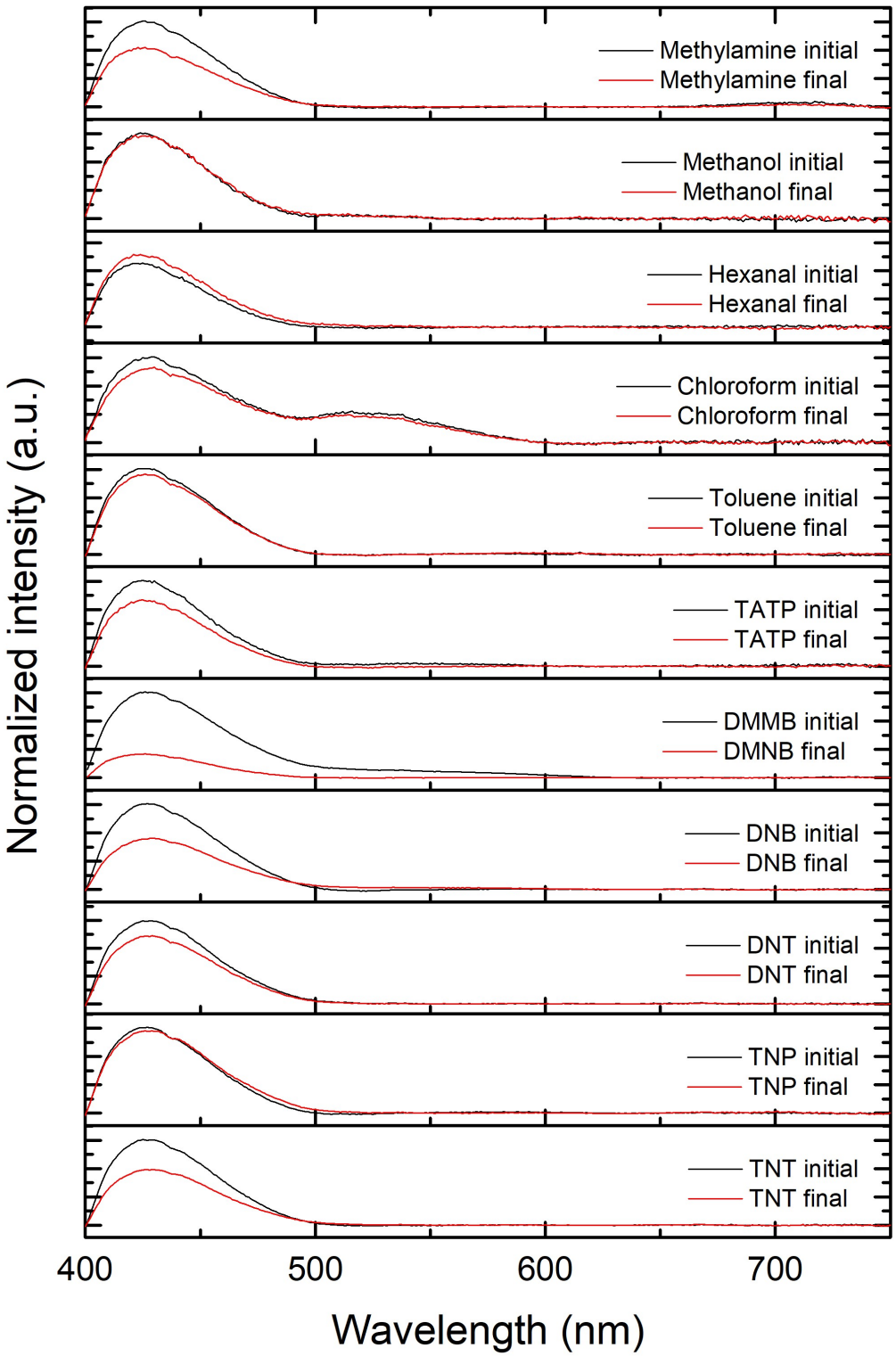

Figure S21: Photoluminescence emission spectra of **UCY-15**(Y)@PDMS films before (black line) and after (red line) exposure to saturated vapours of the indicated analytes.

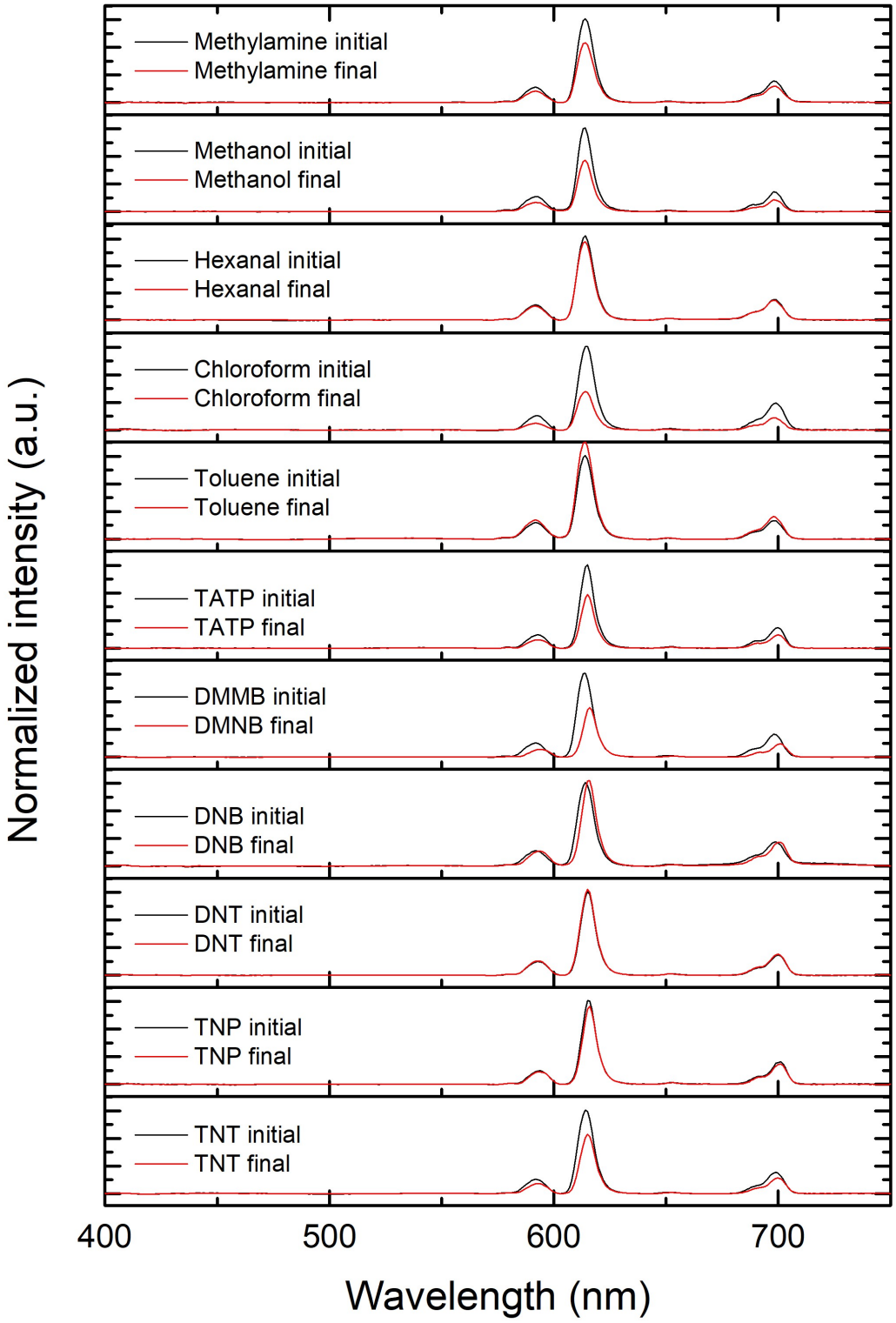

Figure S22: Photoluminescence emission spectra of **UCY-15**(Eu)@PDMS films before (black line) and after (red line) exposure to saturated vapours of the indicated analytes.

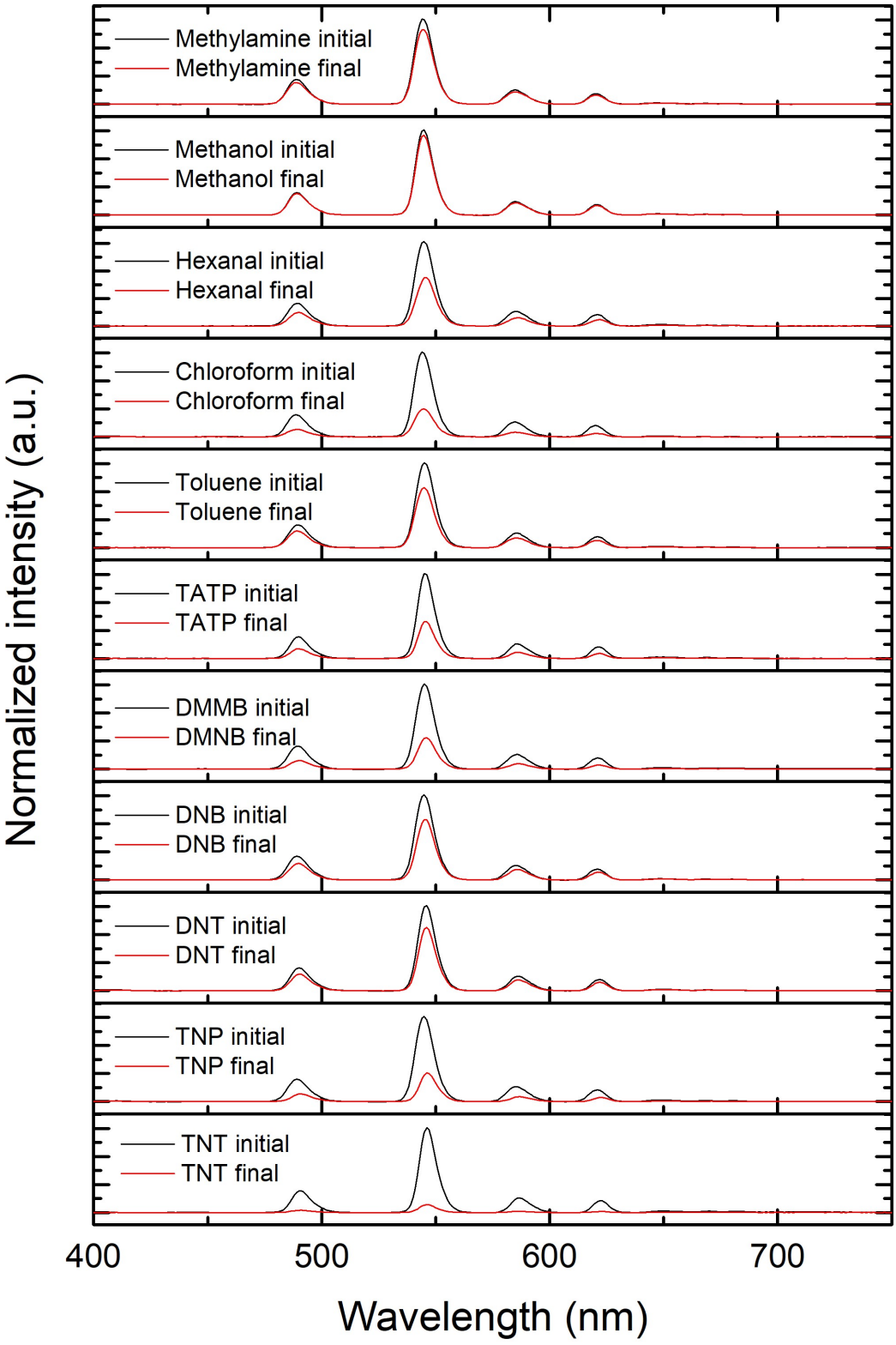

Figure S23: Photoluminescence emission spectra of **UCY-15**(Tb)@PDMS films before (black line) and after (red line) exposure to saturated vapours of the indicated analytes.

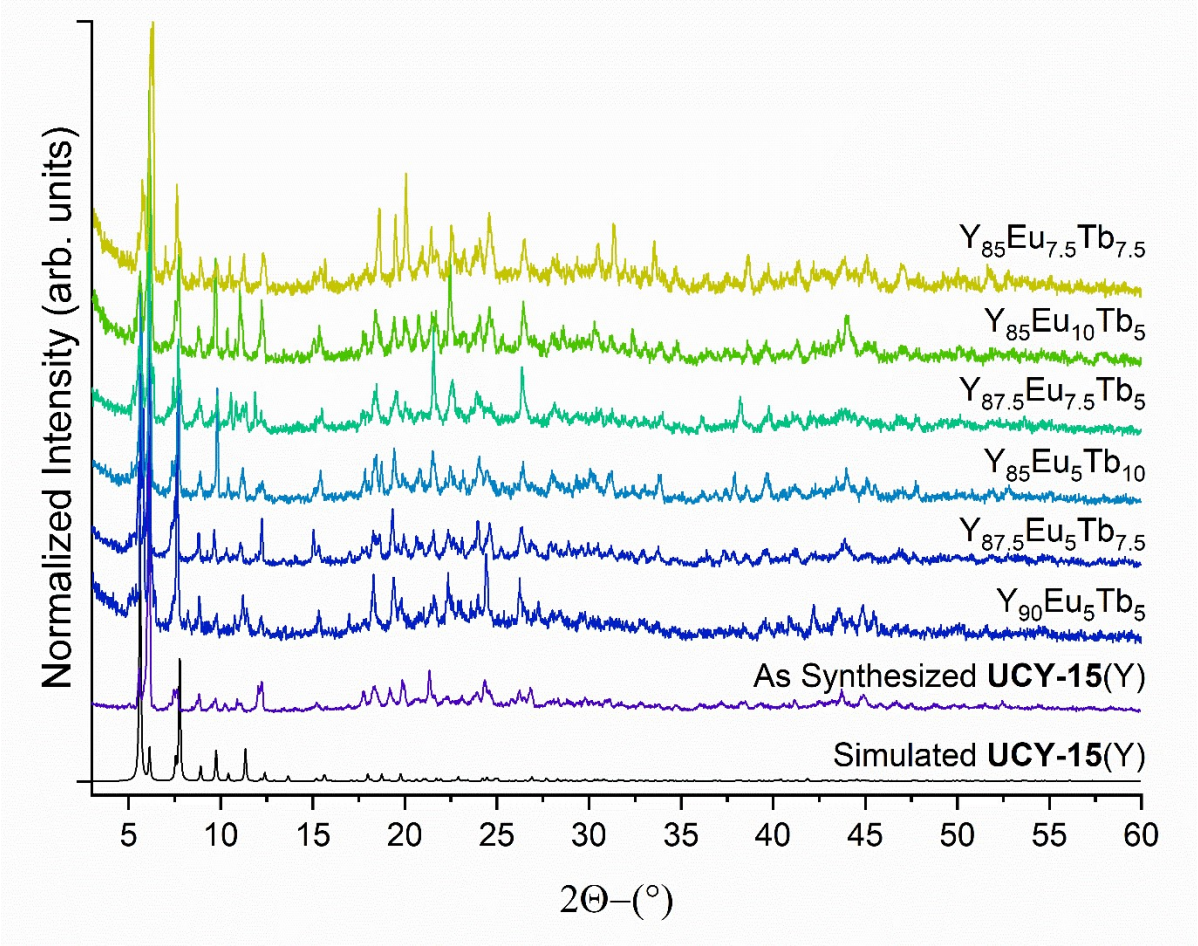

Figure S24: Powder X-ray diffraction patterns of the compound **UCY-15**(Y) and doped analogues **UCY-15**($Y_{100-x-y}Eu_xTb_y$) (x, y = 5, 7.5, 10) along with the simulated pattern from single crystal data of **UCY-15**(Y).

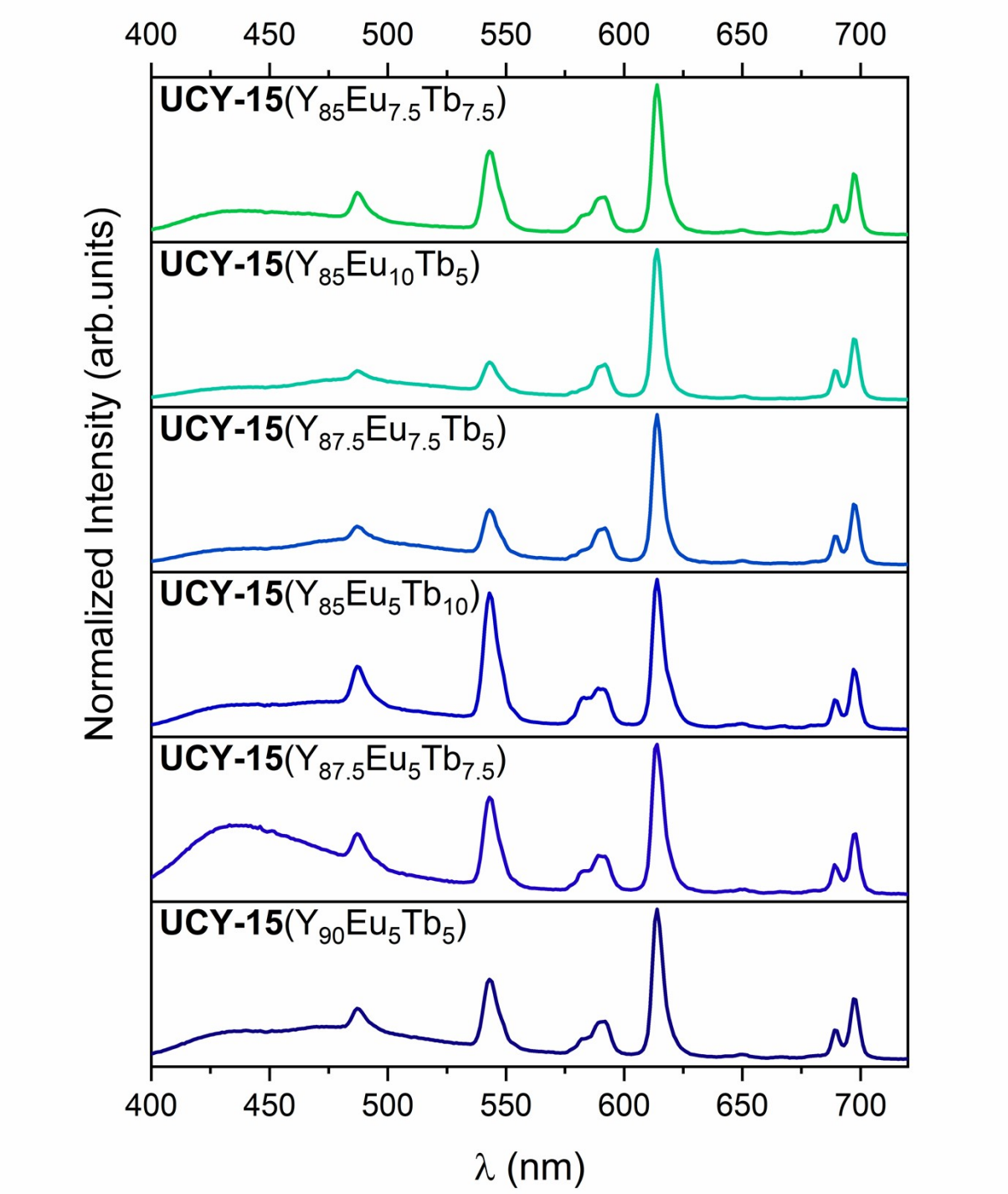

Figure S25: Normalized solid state emission spectra (λ_{exc} = 325 nm) of the as synthesized compounds **UCY-15**($Y_{100-x-y}Eu_xTb_y$) (x, y = 5, 7.5, 10). In each luminescence spectrum a broad band at ~430nm due to $SDBA^{2-}$ emission as well as sharp bands at 578, 591, 613, 651, 699 nm due to $Eu^{3+}$and 487, 543 and 582 nm due to Tb^{3+} ions, are observed.

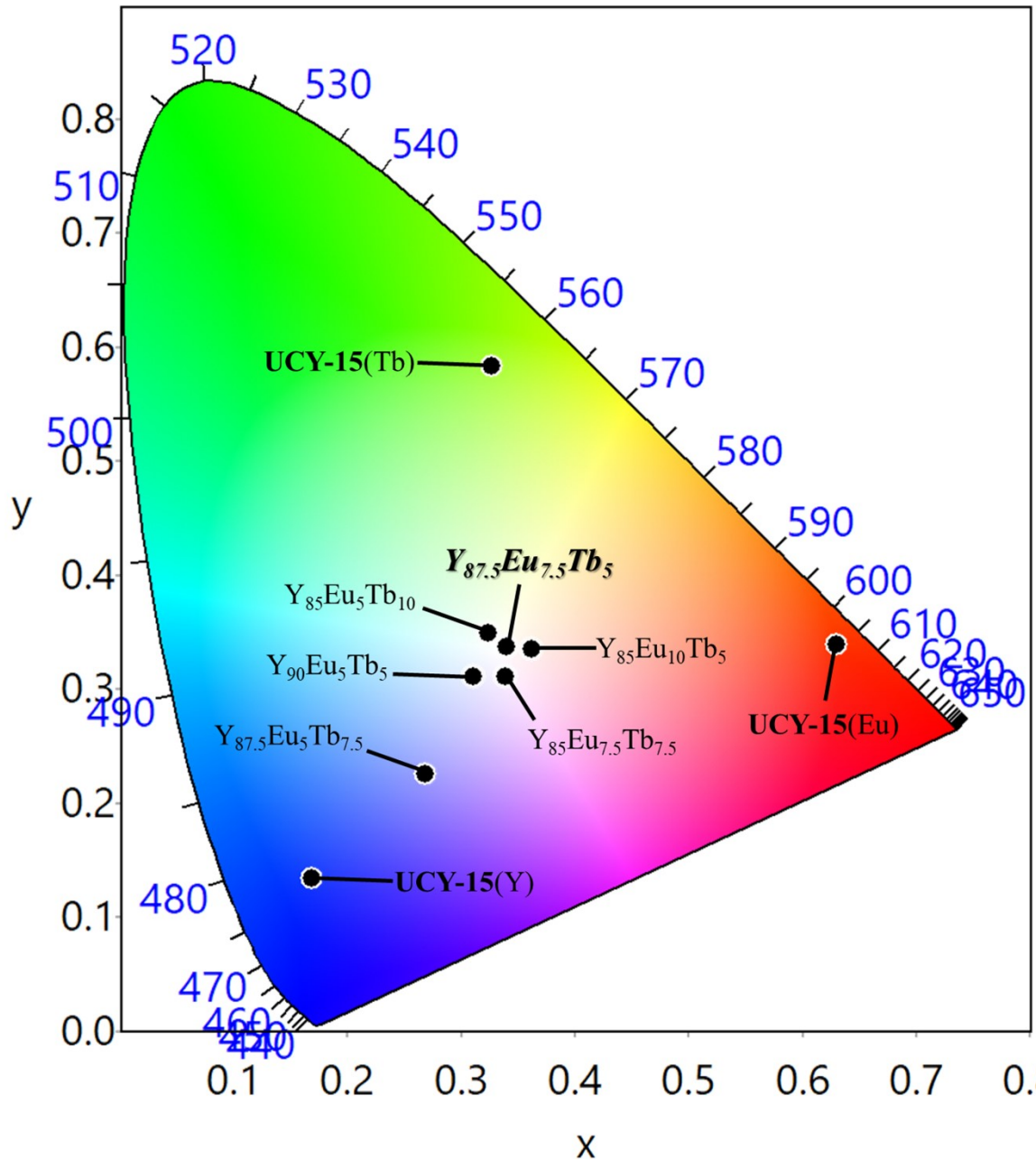

Figure S26: Chromaticity coordinates (CIE 1931) calculated from the corrected emission profiles of **UCY-15**(Y), **UCY-15**(Eu), **UCY-15**(Tb) and **UCY-15**($Y_{100-x-y}Eu_xTb_y$) (x, y = 5, 7.5, 10). This figure shows that the combination of the luminescence from $SDBA^{2-}$, Eu^{3+} and Tb^{3+} results in an analogue emitting white light with coordinates (0.339, 0.337).

Table S4: Chromaticity coordinates of the **UCY-15**($Y_{100-x-y}Eu_xTb_y$) (x, y = 5, 7.5, 10) doped compounds.

Compound	Coordinates	
UCY-15($Y_{100-x-y}Eu_xTb_y$)	x	y
UCY-15($Y_{90}Eu_5Tb_5$)	0.31	0.311
UCY-15($Y_{87.5}Eu_5Tb_{7.5}$)	0.268	0.226
UCY-15($Y_{85}Eu_5Tb_{10}$)	0.324	0.337
UCY-15($Y_{87.5}Eu_{7.5}Tb_5$)	0.339	0.337
UCY-15($Y_{85}Eu_{10}Tb_5$)	0.362	0.335
UCY-15($Y_{85}Eu_{7.5}Tb_{7.5}$)	0.339	0.3108

Figure S27: Digital photographs of **UCY-15**(RE) under a conventional UV lamp operating at 365nm. From left to right: **UCY-15**(Eu), **UCY-15**($Y_{90}Eu_5Tb_5$), **UCY-15**($Y_{87.5}Eu_5Tb_{7.5}$), **UCY-15**($Y_{85}Eu_5Tb_{10}$), **UCY-15**($Y_{87.5}Eu_{7.5}Tb_5$), **UCY-15**($Y_{85}Eu_{10}Tb_5$), **UCY-15**($Y_{85}Eu_{7.5}Tb_{7.5}$) and **UCY-15**(Tb).

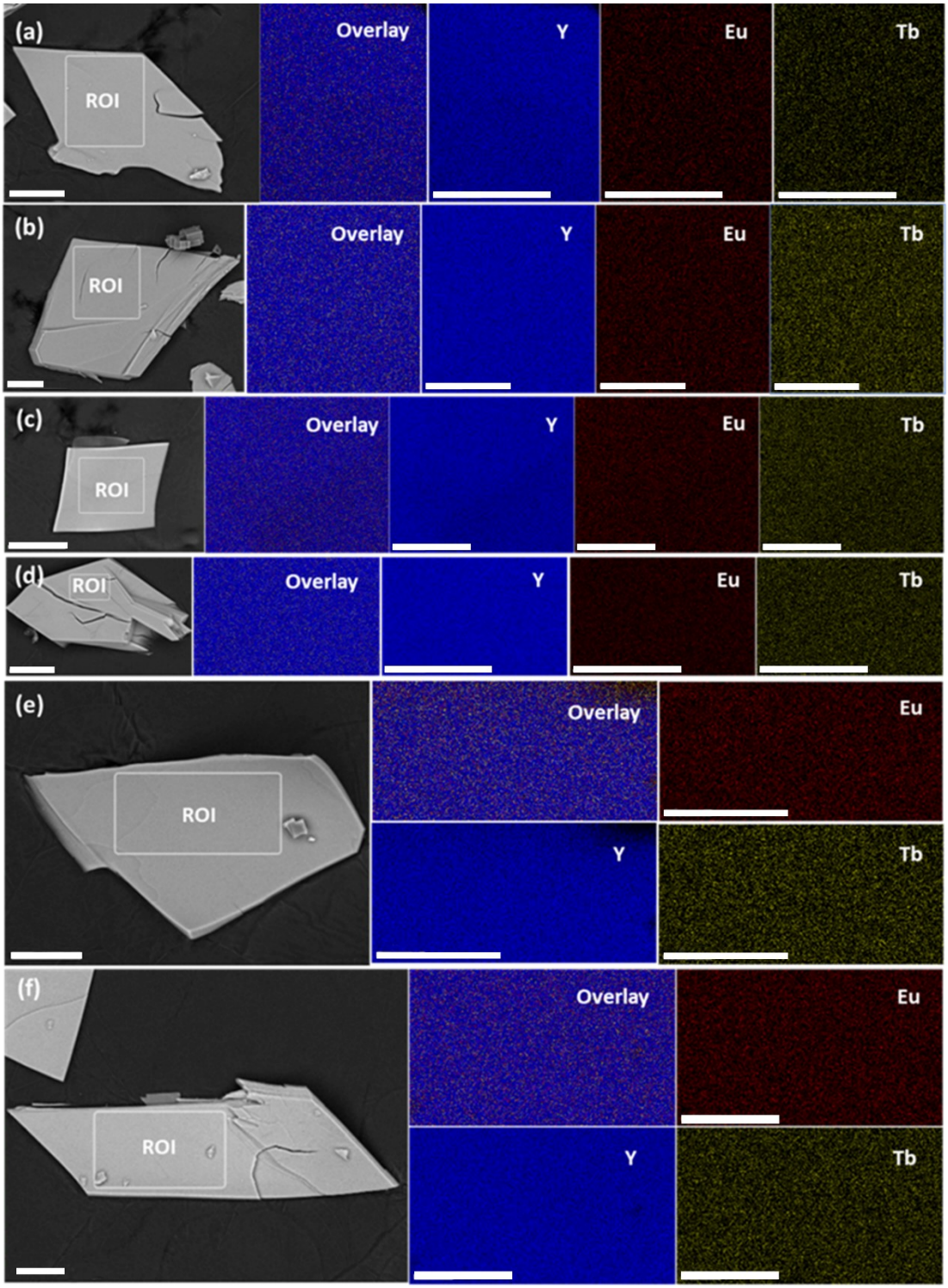

Figure S28: SEM-EDX mapping of UCY-15 samples: a) $Y_{90}Eu_5Tb_5$, b) $Y_{87.5}Eu_5Tb_{7.5}$, c) $Y_{85}Eu_5Tb_{10}$, d) $Y_{87.5}Eu_{7.5}Tb_5$, e) $Y_{85}Eu_{10}Tb_5$ and f) $Y_{85}Eu_{7.5}Tb_{7.5}$. In all cases, the images of the individual metal ions and the overlay correspond to the region of interest (ROI) mapped in the crystal shown in the left images. The equivalence of the scale bar is 50 μm.

Table S5: The (%) ratio of Y^{3+}, Eu^{3+} and Tb^{3+} ions of **UCY-15**($Y_{100-x-y}Eu_yTb_x$) based on EDX results. The error was estimated through the standard deviation (σ) of three independent measurements.

	Theoretical (%)			**Experimental (%)**		
	Y (100-x-y)	**Eu (x)**	**Tb (y)**	**Y**	**Eu**	**Tb**
UCY-15($Y_{90}Eu_5Tb_5$)	90	5	5	90.0±0.1	5±0.5	5±0.1
UCY-15($Y_{87.5}Eu_5Tb_{7.5}$)	87.5	5	7.5	88.7±2.1	5.5±0.8	5.8±0.3
UCY-15($Y_{85}Eu_5Tb_{10}$)	85	5	10	86.0±1.4	5.7±0.8	7.4±1.3
UCY-15($Y_{87.5}Eu_{7.5}Tb_5$)	87.5	7.5	5	87.0±0.1	8.5±1.8	4.8±2.0
UCY-15($Y_{85}Eu_{10}Tb_5$)	85	10	5	84.3±1.5	10.8±1.4	5.2±3.1
UCY-15($Y_{85}Eu_{7.5}Tb_{7.5}$)	85	7.5	7.5	86.0±0.1	7.5±0.7	7.0±0.1

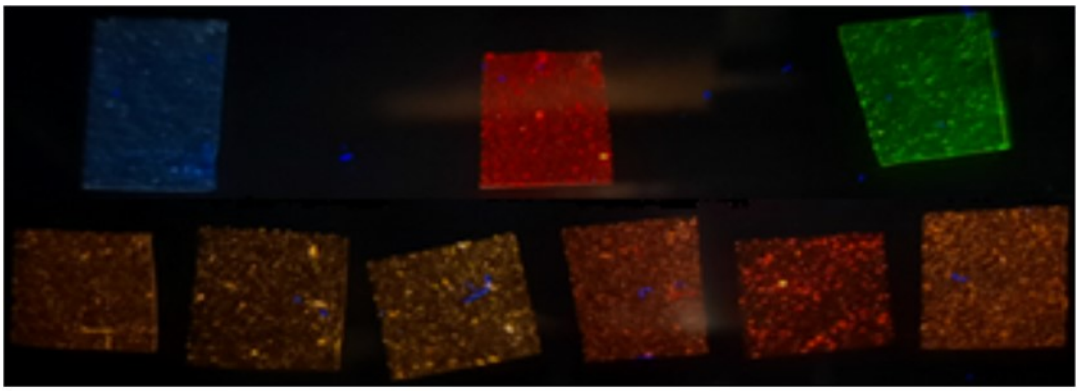

Figure S29: Digital photographs of **UCY-15**(RE)@PDMS films illuminated with UV light (λex=300-375 nm). Top from left to right: **UCY-15**(Y), **UCY-15**(Eu) and **UCY-15**(Tb); bottom from left to right: **UCY-15**($Y_{90}Eu_5Tb_5$), **UCY-15**($Y_{87.5}Eu_5Tb_{7.5}$), **UCY-15**($Y_{85}Eu_5Tb_{10}$), **UCY-15**($Y_{87.5}Eu_{7.5}Tb_5$), **UCY-15**($Y_{85}Eu_{10}Tb_5$) and **UCY-15**($Y_{85}Eu_{7.5}Tb_{7.5}$).

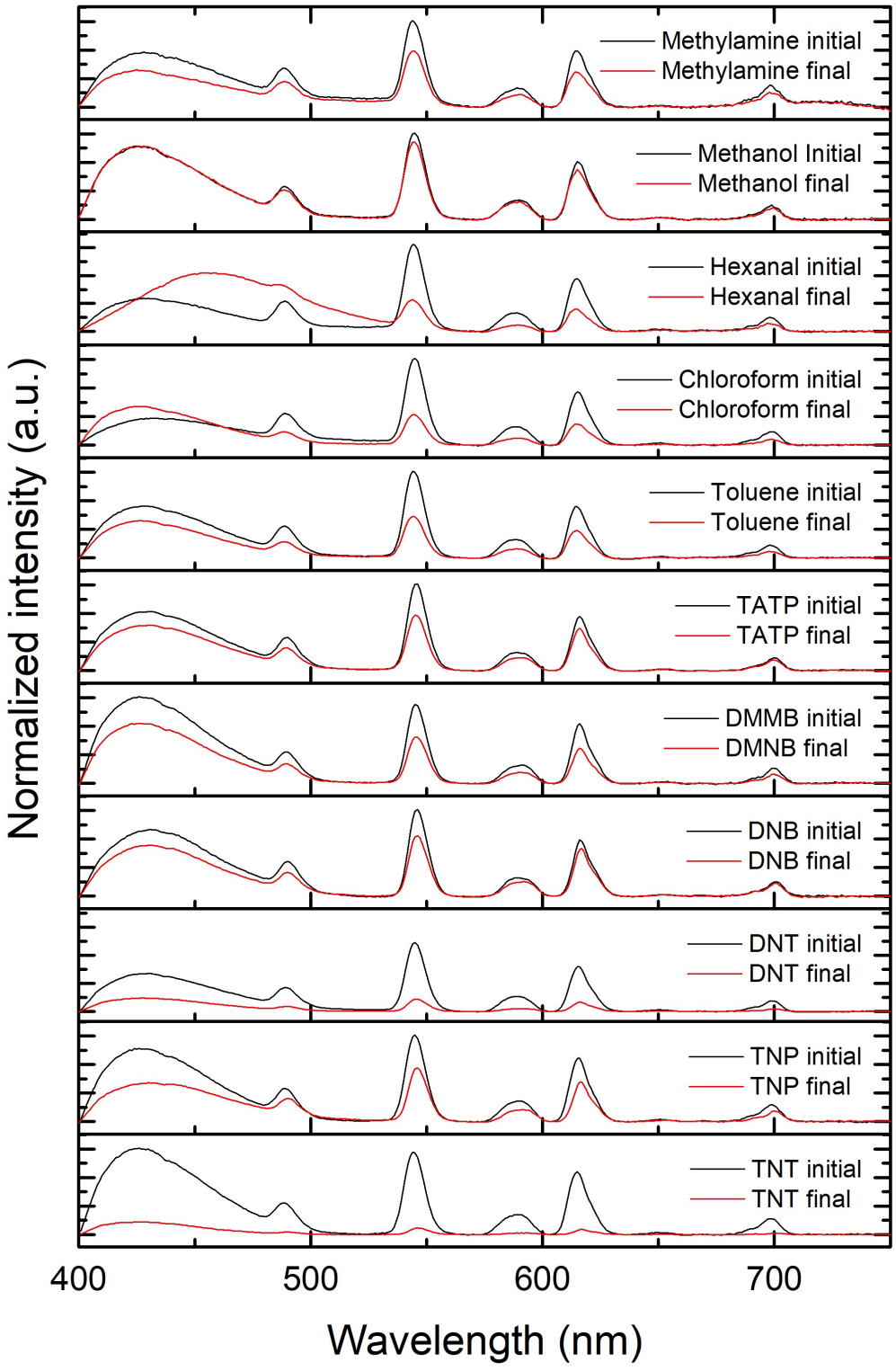

Figure S30: Photoluminescence emission spectra of **UCY-15**($Y_{87.5}Eu_5Tb_{7.5}$)@PDMS before (black line) and after (red line) exposure to saturated vapours of the selected analytes.

Table S6: Relative photoluminescence change (quenching, %) of **UCY-15**($Y_{87.5}Eu_5Tb_{7.5}$)@PDMS upon exposure to the different nitro-compounds. The concentration (v/v) was calculated at room temperature (25ºC).

Analyte	**Gas concentration[3]**	**Quenching (%)**	**Normalized response (ppb^{-1})**
TNT	7.23 ppb	78	10.8
TNP	0.98 ppb	16.9	17.2
DNT	346 ppb	82	0.2
DNB	1.16 ppm	30	0.03
DMNB	2.59 ppm	24.5	0.01

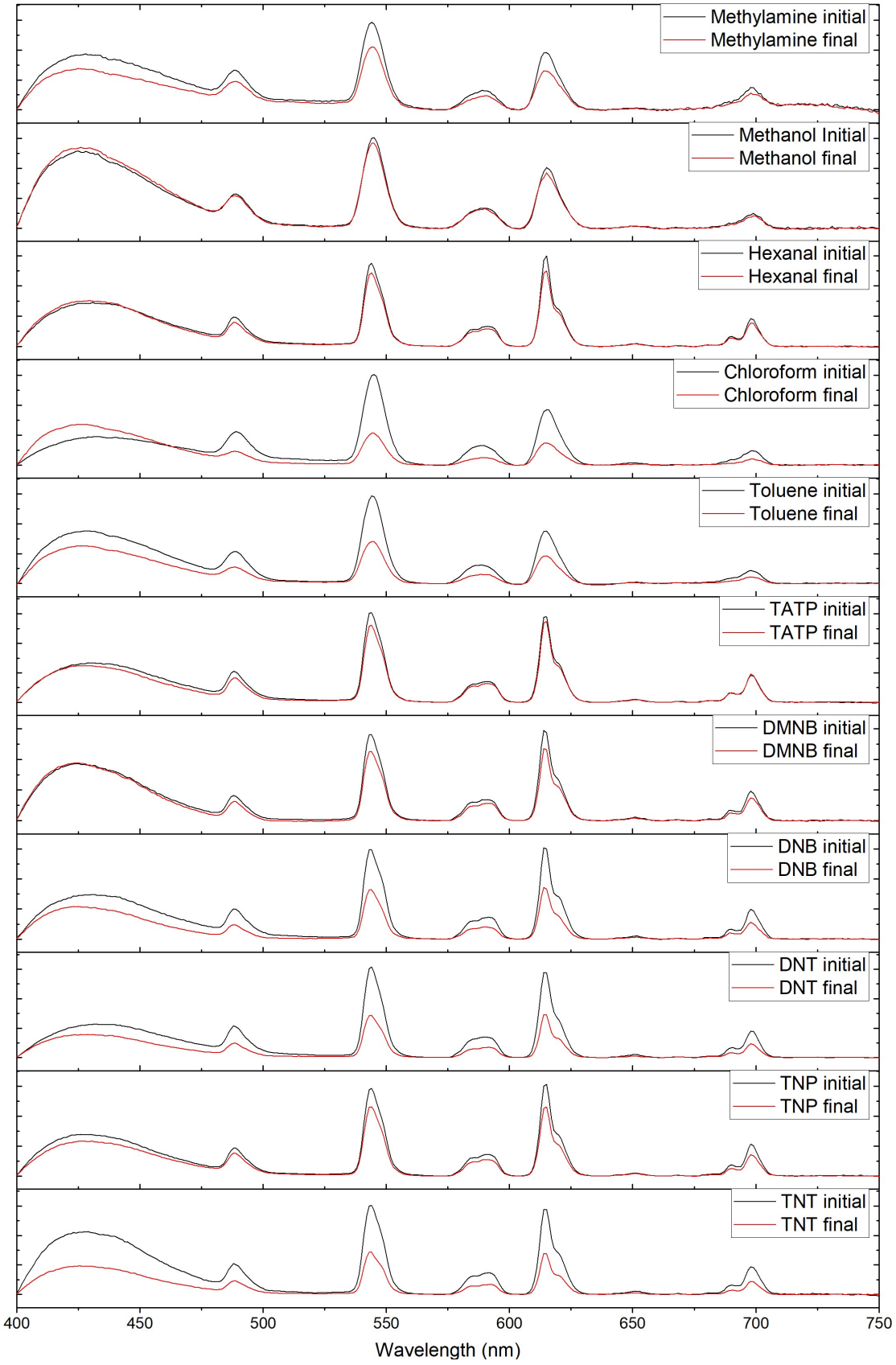

Figure S31: Photoluminescence emission spectra of **UCY-15**($Y_{87.5}Eu_5Tb_{7.5}$)@PDMS before (black line) and after (red line) 5 min exposure to saturated vapours of the selected analytes.

References

1. S. Park, J. Lee, S. G. Cho, E. M. Goh, S. Lee, S.-S. Koh and J. Kim, Mass Spectrometric Analysis of Eight Common Chemical Explosives Using Ion Trap Mass Spectrometer, *Bull. Korean Chem. Soc.*, 2013, **34**, 3659.

2. G. R. Peterson, W. P. Bassett, B. L. Weeks and L. J. Hope-Weeks, Phase pure triacetone triperoxide: The influence of ionic strength, oxidant source, and acid catalyst, *Cryst. Growth Des.*, 2013, **13**, 2307.

3. J. P. Vizuet, M. L. Mortensen, A. L. Lewis, M. A. Wunch, H. R. Firouzi, G. T. McCandless and K. J. Balkus, Fluoro-Bridged Clusters in Rare-Earth Metal–Organic Frameworks, *J. Am. Chem. Soc.*, 2021, **143**, 17995.

4. K. O. Christe and W. W. Wilson, Nuclear magnetic resonance spectrum of the fluoride anion, *J. Fluor. Chem.*, 1990, **46**, 339.

5. W. He, F. Du, Y. Wu, Y. Wang, X. Liu, H. Liu and X. Zhao, Quantitative 19F NMR method validation and application to the quantitative analysis of a fluoro-polyphosphates mixture, *J. Fluor. Chem.*, 2006, **127**, 809.

6. L. Czepirski and J. JagieŁŁo, Virial-type thermal equation of gas—solid adsorption, *Chem. Eng. Sci.*, 1989, **44**, 797.

7. K. Sumida, D. L. Rogow, J. A. Mason, T. M. McDonald, E. D. Bloch, Z. R. Herm, T.-H. Bae and J. R. Long, Carbon Dioxide Capture in Metal–Organic Frameworks, *Chem. Rev.*, 2012, **112**, 724.

8. M. H. V Werts, R. T. F. Jukes and J. W. Verhoeven, The emission spectrum and the radiative lifetime of Eu3+ in luminescent lanthanide complexes, *Phys. Chem. Chem. Phys.*, 2002, **4**, 1542.

9. N. M. Shavaleev, S. V Eliseeva, R. Scopelliti and J.-C. G. Bünzli, N-Aryl Chromophore Ligands for Bright Europium Luminescence, *Inorg. Chem.*, 2010, **49**, 3927.